# UNIVERSITY OF TURKU

## Faculty of Science and Engineering

# The activation of the Rig-I pathway after sendai virus infection in A549 cells

University of Turku
Faculty of Science and
Engineering
MSc Thesis
Department of Biology
May 2020
Jemna Heroum

Supervisors: Pekka Kolehmainen,
Ilkka Julkunen, and Harri Savilahti

The originality of this thesis has been checked in accordance with the
University of Turku quality assurance system using the Turnitin Originality
Check service

---

Sendai virus (SeV) is a single-stranded negative-sense RNA virus belonging to the family *Paramyxoviridae*. It is an important model and vector virus, and a murine pathogen. Innate immunity is the first to act on infections. Invading viruses are recognized by pattern recognition receptors (PRRs) belonging to innate immunity. Retinoic-acid inducible gene-1 (Rig-I) is one key cytosolic PRR and recognizes primarily short double-stranded RNA. Activation of the Rig-I pathway leads to the activation of the transcription factor interferon regulatory factor 3 (IRF3). Activated IRF3 translocates from cytoplasm into the nucleus. There it regulates the production of interferons (IFNs) and other pro-inflammatory molecules aiming to eliminate the virus. In this study, the activation kinetics of the Rig-I pathway were studied *in vitro* in A549 cells infected with SeV Cantell strain. The central interest was the activation requirements of the Rig-I: whether innate immunity responses are activated when the virus is not replicating. IRF3 movement, *IFN-β1* and *IFN-λ1* and SeV *N* gene mRNA expressions, and host and viral protein expressions in the infected cells were studied by immunocytochemical staining, qRT-PCR, and immunoblotting. In addition, experiments with cells treated with cycloheximide (CHX), which inhibits protein synthesis, were done. Interestingly, the results demonstrate that the Rig-I pathway activation occurred by one hour after the SeV-infection followed by effective IFN mRNA expressions between two and four hours after the SeV-infection, and these were independent of the virus replication. Consequently, it is enough that SeV enters the cell, without the virus replication, to be recognized and elicit antiviral responses.

---

KEYWORDS: Sendai virus, virus replication, Rig-I pathway,

interferons, innate immunity

# Contents

# 1. Introduction

## 1.1 What are viruses?

Viruses are tiny packages of genetic information (Koonin et al. 2015). Unlike other biological entities, viruses are incapable of replicating themselves (Walsh and Mohr 2011). Thus, they are obligate parasites that invade, i.e. infect, a cellular host organism and exploit its metabolic machinery to replicate and produce the needed components to amass progeny viruses (Walsh and Mohr 2011). Viruses are a diverse group of particles: they exist in different shapes, sizes, and structures (Koonin et al. 2015). In fact, when surveying the whole virus genera, universally found gene(s) of all viruses lacks (Koonin et al. 2006). However, there are some hallmark viral genes that are shared among certain group of viruses and are lacking in cellular organisms (Koonin et al. 2006). Nonetheless, there are some unifying structures and functioning mechanisms, particularly within a certain taxonomic group (Tordo et al. 1988; Poch et al. 1989).

First, all viruses have some kind of capsid structure, which encapsulates and protects the viral genome creating a nucleocapsid (Koonin et al. 2006; Mateu 2013). Since the capsid protects the viral genome, maintaining the proper form and function of the capsid is vital for keeping the virus infective (Mateu 2013). On the other hand, it must be a labile structure and able to be disrupted in order to release the virus genome into the cytosol after the virus has entered the host cell (Mateu 2013).

Some viruses have another protecting layer on top of the capsid: an envelope (Plemper 2011). Unenveloped viruses comprise of only the nucleocapsid structure. Enveloped viruses have a lipid (bi)layer that has proteins embedded in it (Plemper 2011). The envelope of a virus has also other important roles than purely protective. Proteins in the envelope mediate the virus entry into the host cell (Scheid and Choppin 1974; Bousse et al. 1994; Bitzer et al. 1997, Plemper 2011). Significant differences, in both function (Matlin et al. 1981; Moscufo et al. 1993; Liemann et al. 2002) and sensitivity (Shirai et al. 2000; Kramer et al. 2006; Thevenin et al. 2013; Firquet et al. 2015), appear between the enveloped and non-enveloped viruses. The ones

that possess an envelope are generally easier to degrade since the envelope comprises of lipid layers, and detergents can therefore easily interfere their integrity (Shirai et al. 2000; Thevenin et al. 2013).

All of the life domains, eukarya, archaea, and bacteria, are threaten by viruses' capability to infect (Koonin et al. 2015). Even viruses themselves can be infected by a virus (La Scola et al. 2008). Each virus has a certain host cell range that it infects, for example bacteriophages only infect specific bacterial cells (Koonin et al. 2015). The virus's interaction with the host cell and adsorption ability is dependent on the receptors expressed on the virus and the host cell surface (Markwell and Paulson 1980; Deng et al. 1996; Chu and Whittaker 2004). Therefore, this possible host cell range is further limited, since different cell types express dissimilar receptors on their surfaces (Zhu et al. 2011).

In general, viruses can have deoxyribonucleic acid (DNA) or ribonucleic acid (RNA) genome, of which both can be either single-stranded (ss) or double-stranded (ds) (Baltimore 1971; Agol 1974). In each of these combination alternatives, the genome can be circular or linear (Baltimore 1971; Agol 1974). Furthermore, the genome can be segmented or not, meaning that the genome is in pieces or as a continuous fragment, respectively (Baltimore 1971; Agol 1974). RNA genomes are generally further divided into negative- or positive-sense RNAs (Baltimore 1971; Agol 1974). The difference between these two groups is that positive-sense RNA can directly act as an mRNA template for translation, but negative-sense RNA requires an additional step before it can be translated into viral proteins (Baltimore 1971; Agol 1974). That is, first it needs to be transcribed into positive-sense, i.e. antisense, mRNA.

## 1.2 Sendai virus

Sendai virus (SeV), also known as hemagglutinating virus of Japan (HVJ) or mouse parainfluenza virus type 1, belongs to the family *Paramyxoviridae* and in the genus *Respirovirus* (Afonso et al. 2016). The family *Paramyxoviridae* includes also significant human pathogens such as respiratory syncytial virus (RSV) and human metapneumovirus (HMPV) (Afonso et al. 2016). Sendai virus is a single-stranded, negative-sense RNA virus, and has an envelope (Faísca and Desmecht 2007). The viral genome, which is around 15 kb in

size, is non-segmented (Faísca and Desmecht 2007). SeV genome consists of six genes that code for six structural proteins. The six virus genes are located in tandem and ordered so that N protein is the first from the 3' end followed by P, M, F, HN, and lastly at the 5' end L (Faísca and Desmecht 2007) (Figure 1).



Figure 1. Negative strand RNA genome of sendai virus. Modified from Cox and Plemper (2015).

The *P* gene of SeV is polycistronic meaning that it codes for more than one protein from the single mRNA via multiple overlapping open reading frames (ORFs) (Dethlefsen and Kolakofsky 1983; Curran and Kolakofsky 1988). Thus, the *P* gene can result in different translational products that are non-structural, i.e. that are lacking in the virion structure, C proteins (C and C'), P protein, non-structural Y protein (Curran and Kolakofsky 1988), and V protein (Kato et al. 1997). This mRNA editing happens by insertion of a guanidine to a specific place in the mRNA thus creating a frameshift and ultimately another protein (Vidal et al. 1990). At the 3' and 5' ends of the genome lie small regions called leader (*le*) and trailer (*tr*), respectively (Leppert et al. 1979; Kolakofsky et al. 2004). The positions of these regions are also visualized in the Figure 1. *Le* and *tr* are both noncoding regions (Kolakofsky et al. 2004). The *le* region is the promoter for the synthesis of mRNA as well as for the intermediate, positive-sense antigenome (Kolakofsky et al. 2004). At the 3' end of the antigenome (at the 5' end of the genome) is the *tr* region, which directs the synthesis of the genome (Noton and Fearns 2015). The antigenome serves as a template for the negative-sense genome, which is the final product of the virus genome replication (Kolakofsky et al. 2004).

SeV nucleocapsid (N) protein's N-terminal domain is in charge of encapsulation of the virus genome and of the assembly of the virus nucleocapsid (Buchholz et al. 1993). The SeV nucleocapsid is formed, to a lesser extent, of two other components as well: the large (L) protein and the phosphoprotein (P) (Portner et al. 1988). Like noted, SeV has negative-sense, single-stranded RNA genome and the RNA is tightly encapsulated by N protein forming the nucleocapsid structure (Faísca and Desmecht 2007). To start the replication, the virus first needs to enter the cell and release its

genome into the cytosol (Vabret and Blander 2013). Paramyxovirus genome transcription and replication (Figure 2) are complicated processes, and much is still unknown (Kolakofsky et al. 2004). The basic principles of these are covered further in the chapter.
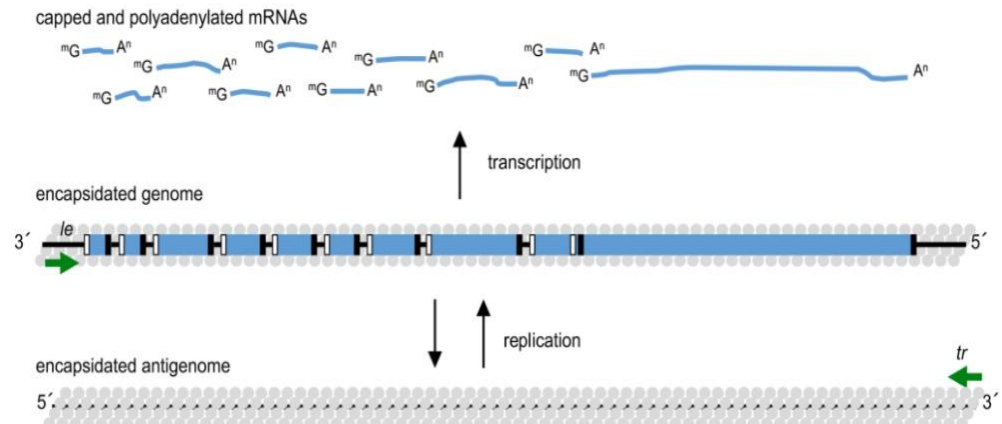


Figure 2. SeV (-)ssRNA genome structure and its transcription and replication. Modified from Noton et al. (2019).

The template for transcription is the nucleocapsid rather than free RNA (Myers and Moyer 1997). The negative-sense RNA is transcribed into subgenomic mRNAs by the virus RNA-dependent RNA polymerase (RdRP) (Kolakofsky et al. 2004). Biologically active RdRP of SeV is a complex of the L and P proteins, and this RNA polymerase requires nucleocapsid association to function (Horikami et al. 1992; Smallwood et al. 1994). The RdRP recognizes from *gene start and gene end* signals, short sequences in both sides of the ORF, where to start and stop the transcription, respectively (Kolakofsky et al. 2004). The mRNAs have 5' methyl caps (Ogino et al. 2005) and 3' polyadenylated structures (Pridgen and Kingsbury 1972; Murphy and Lazzarini 1974 a study made with vesicular stomatitis virus (VSV)). When the polymerase encounters a *gene end* signal, it stops the transcription (Kolakofsky et al. 2004). Then the above-mentioned mRNA modifications are performed, after which the mRNA is released (Iverson and Rose 1981 a study made with VSV; Kolakofsky et al. 2004; Noton and Fearns 2015). After releasing the formed mature mRNA, the RNA polymerase continues to scan along the gene junctions, i.e. intergenic, noncoding regions, and produces a new mRNA when it finds a new *gene start* signal (Noton and Fearns 2015). When the amount of soluble N protein ($N_0$) mRNA has risen to a certain level, transition from transcription to replication can start (Curran et al. 1995). This transition is explained by the fact that the $N_0$, which is associated with N-

terminal domain of the P protein (and thus soluble and unassembled), is required for the assembly and encapsulation of the nascent chain in genome replication (Curran et al. 1995). Irie et al. (2014) have proposed that SeV C protein dictates the shift from positive (mRNAs and antigenome) to negative (genome) transition. This idea is based on C protein mutation experiments by Irie et al. (2014), which show C protein being capable of inhibiting leader genome promoter (GP) when the amount of C protein reaches a certain threshold value as the infection proceeds (Irie et al. 2014). However, C protein is incapable of inhibiting trailer antigenome promoter (AGP) (Irie et al. 2014). In short, the mRNAs and antigenome are produced and then the switch to produce full-length negative-sense genome occurs since accumulated C proteins suppress the GP (Irie et al. 2014).

The virus RdRP is also responsible for the replication of the genome. Altogether, N, L, and P proteins have been shown to be necessary for the SeV genome replication *in vivo* (Curran et al. 1991). In the replication phase, the RdRP elongates the template genome to produce complete length positive sense antigenome by ignoring the gene junctions, so that no incomplete and modified mRNAs are released (Noton and Fearns 2015). The antigenome and genome RNA ends lack the cap structure but are instead associated with the N protein (Noton and Fearns 2015). The genome synthesis and the encapsulation of the genome by N protein happen concomitantly (Gubbay et al. 2001). The encapsulated genomes are then assembled into new virions and at the last step of the life cycle, they bud out of the host cell ready to infect new hosts (Faísca and Desmecht 2007).

The matrix (M) protein and C protein of SeV are linked to the budding of new virions from the host cell (Irie et al. 2007; Irie et al. 2008). Additionally, the Fusion (F) protein has been linked to the budding process of new virions (Takimoto et al. 2001). The SeV C protein has numerous other functions than just enhancing the budding of newly formed viruses. Horikami et al. (1997) showed that SeV C protein can bind the virus L protein, which is the catalytic domain of the virus RdRP, and by doing that it can regulate the viral RNA synthesis. In addition, SeV C proteins are shown to possess anti-apoptotic activity (Koyama et al. 2003) as well as ability to inhibit innate immunity responses by interfering the interferon production and signaling (Kato et al. 2001; Kato et al. 2004; Komatsu et al. 2004).

On the surface of the virion, and more specifically on the virus envelope, is F protein, which aids the virus particle to fuse with the host cell membrane (Scheid and Choppin 1974; Tanabayashi and Compans 1996; Bitzer et al. 1997). The F protein of paramyxoviruses is in an inactive state when the virus is without interaction with a host cell and needs to be cleaved to achieve biologically active form capable of assisting the entry into host cell (Scheid and Choppin 1974; Bitzer et al. 1997). The cleaved, active form of paramyxovirus F protein is structured of two subunits: $F_1$ and $F_2$ (Scheid and Choppin 1974). Tashiro et al. (1990) found that proteolytic cleavage of SeV F protein occurred to the most part in lung tissue. The cleavage of the precursor $F_0$-protein can be mediated also with trypsin treatment in cell cultures (Scheid and Choppin 1974). Additionally, Kido et al. (1992) found a protease that resembles trypsin (Tryptase Clara) and that is only expressed in bronchiolar epithelial Clara cells purified from rat lungs and concluded that the protease could be responsible for activating precursor viral fusion proteins. Eliciting SeV fusion to the host cell membrane has been shown to require also the other envelope glycoprotein, the hemagglutinin-neuraminidase (HN) protein (Bousse et al. 1994; Tanabayashi and Compans 1996). HN-protein function also in the attachment of SeV to the host cell by interacting with the host's receptors that contain sialic acid (Markwell and Paulson 1980).

Sendai virus infects naturally mice and to minor extent other rodents such as rats (Ishida and Homma 1978). Bronchial epithelial cells are the prime targets of SeV infection (Ishida and Homma 1978). Experimentally it is yet possible to infect cell lines from other origins, including humans. Viruses can cause a cytopathic effect to the host cell. For example, SeV infected cells can fuse together and form a giant polykaryocyte cell (Okada et al. 1966). In addition, other morphological changes in infected cells take place and can be observed microscopically. In experimental settings, adherent cells can for example become rounder and shrink after infection and eventually detach from the growth plate surface and die (Matsumoto and Maeno 1961). Symptoms related to SeV include rhinitis, anorexia, destruction of respiratory tract epithelium, bronchiolitis, and pneumonia (Ishida and Homma 1978). In a majority of cases SeV infection leads to death of the host (Ishida and Homma 1978). A vaccine against SeV is lacking.

## 1.3 Innate immunity

Immune system works in keeping the host pathogen-free and in case this fails, in activating responses that lead to eradication of the pathogen (Medzhitov 2007). Immune system has been developed early in evolution, and some of its fundamental characteristics are conserved in animal kingdom from vertebrates to invertebrates (Medzhitov et al. 1997; Chaudhary et al. 1998; Rock et al. 1998; Sanghavi et al. 2004). In vertebrates, immunity is subdivided into innate and adaptive immunity (Medzhitov 2007). They work in co-operation but have dissimilar features (Medzhitov 2007). Innate immunity acts rapidly and non-specifically against new pathogens (Medzhitov 2007). It produces no memory like adaptive immunity, which relies on formation of memory and specific responses via production of antibodies by B-cells and via functions of different T-cell populations (Medzhitov 2007). The production of antibodies and activation of T-cells is ultimately modulated by the quality and form of the innate immunity responses (Fritz et al. 2007; Medzhitov 2007).This is so, because naïve T-cells are primed based on the cytokine cocktail produced by the innate immune antigen presenting cells (APCs), which in turn are evolving based on the cytokines innate immune reaction produces (Medzhitov et al. 1997; Fritz et al. 2007; Medzhitov 2007). Therefore, proper activation of innate immunity also contributes to efficient development of adaptive immunity (Medzhitov et al. 1997; Fritz et al. 2007; Medzhitov 2007).

Innate immunity is the initial system to react to infections (Medzhitov 2007). Physical barriers like skin and respiratory tract epithelium function as first line defenses against pathogens (Medzhitov 2007). They function as a mechanic shield but also by producing antimicrobial peptides (Medzhitov 2007). For instance, skin keratinocytes and lung epithelium cells have been shown to produce an antimicrobial agent, β-defensin-3 (hBD-3), which is shown to kill several different pathogens (Harder et al. 2001). Innate immunity is based on a large and complex system. Cellular components that belong to that are the complement system and specific leukocytes (Medzhitov 2007). These leukocytes include natural killer cells, basophils, eosinophils, neutrophils, and monocytes as well as macrophages and dendritic cells, which both derive from monocytes (Medzhitov 2007). However, in addition to leukocytes, many different cell types possess the ability to react and modulate immunity: for example, human lung epithelial cells and human

keratinocytes can produce some of the type I interferons (IFNs) (LaFleur et al. 2001; Jewell et al. 2007).

Invading pathogens are recognized by pathogen associated molecular patterns (PAMPs) that are lacking in the uninfected cells and the recognition occurs by pattern recognition receptors (PRRs) (Medzhitov 2007). Recognition of a PAMP ultimately leads to activation of the host innate immunity responses, like IFN production (Medzhitov 2007). There are many different protein families of germline-encoded PRRs (Medzhitov 2007). These receptors can be found in the surface of the cell or in endosomal compartments (Medzhitov 2007). When they are located such, they are transmembrane receptors (Medzhitov 2007). In addition, they can be found in the cytosol being then intracellular (Medzhitov 2007). Retinoic-acid inducible gene 1 (Rig-I) like receptors, Toll-like receptors (TLRs), and protein kinase R (PKR) belong to some of the main receptors regulating innate immunity responses in virus infections (Mogensen and Paludan 2005; Meylan et al. 2006). For example, lipopolysaccharide (LPS) is a PAMP and it is recognized by TLR4 (Hoshino et al. 1999) that is a PRR, which then activates innate immunity. Other examples are bacterial flagellin (PAMP) which is recognized by TLR5 (PRR) (Hayashi et al. 2001), fungal β-Glucan (PAMP) which is recognized by Dectin-1 (PRR) (Taylor et al. 2007), or viral RNA (PAMP) which is recognized by Rig-I (PRR) (Yoneyama et al. 2004).

Importantly, PRRs lack specificity to pathogens, so they can recognize a wide range of pathogens that have some unifying molecular structure or motif (Medzhitov 2007). On the other hand, adaptive immunity relies on recognizing an infinite number of different antigens by specific B- or T-cell receptors (Medzhitov 2007). Additionally, PRRs do not distinguish whether the micro-organism is pathogenic or non-pathogenic (Medzhitov 2007). For example, TLRs recognize also symbiotic bacteria residing for example in the human gut, and this has been shown to be beneficial and essential for the intestinal epithelial homeostasis (Rakoff-Nahoum et al. 2004). TLRs are perhaps the best known PRRs by to date, and there are ten different human TLRs described (Mogensen and Paludan 2005). The receptor mechanisms are not fully understood, and the receptors can cooperate with one another (Ozinsky et al. 2000).

As described in this chapter, host PRRs are an important part of the innate immunity and can recognize certain abnormal molecular structures present in the cell. PRRs may also recognize host's own structures and therefore cause autoimmune diseases (Medzhitov 2007). This thesis work focuses on the Rig-I pathway activated by sendai virus infection. Therefore, in the next chapter, the Rig-I PRR pathway is described in more detail.

1.4 The Rig-I signaling pathway in virus infections

When virus has entered the host cell it is recognized through PRR (Akira et al. 2006). Rig-I is a cytosolic RNA helicase PRR that belongs to Rig-I-like receptor family (RLR) and is a significant part of cellular innate immunity in viral infections (Yoneyama et al. 2004; Saito et al. 2007). To the same family with Rig-I belongs also melanoma differentiation-associated gene 5 (MDA5) (Akira et al. 2006). Contrary to RLRs, TLRs are located either on the surface of a cell or inner surface of an endosome, i.e. they are membrane bound structures in the cytosol (Mogensen and Paludan 2005). Therefore, foreign structures in endosomes and outside the cell or in cytosol can be recognized either by TLRs or RLRs, respectively (Mogensen and Paludan 2005). Hence, depending on the compartment where the virus replicates, cytosol or nucleus, only particular PRRs can mediate the antiviral signal (Beachboard and Horner 2016). This is also proven by a study of Liu et al. (2018) where they found a counterpart for the cytosolic Rig-I in the nucleus: the nuclear Rig-I was capable of recognizing influenza A virus (IAV) that replicates in the nucleus but incapable of recognizing SeV that replicates in the cytosol. Moreover, if the invading virus is concealing its genomic material inside an intracellular membrane, like dengue virus (DENV) and IAV, its recognition is delayed and possibly inaccessible to RLRs (Österlund et al. 2012; Uchida et al. 2014). The mechanism that the incoming virus uses to entry the host cell, for example fusion or endosomal route, further sets limitations on the PRR that recognizes it (Akira et al. 2006; Österlund et al. 2012; Wu and Chen 2014).

An overview of the structures of the Rig-I and MDA5 receptors and some of the steps and complexes involved in these signaling pathways are presented in figure 3.
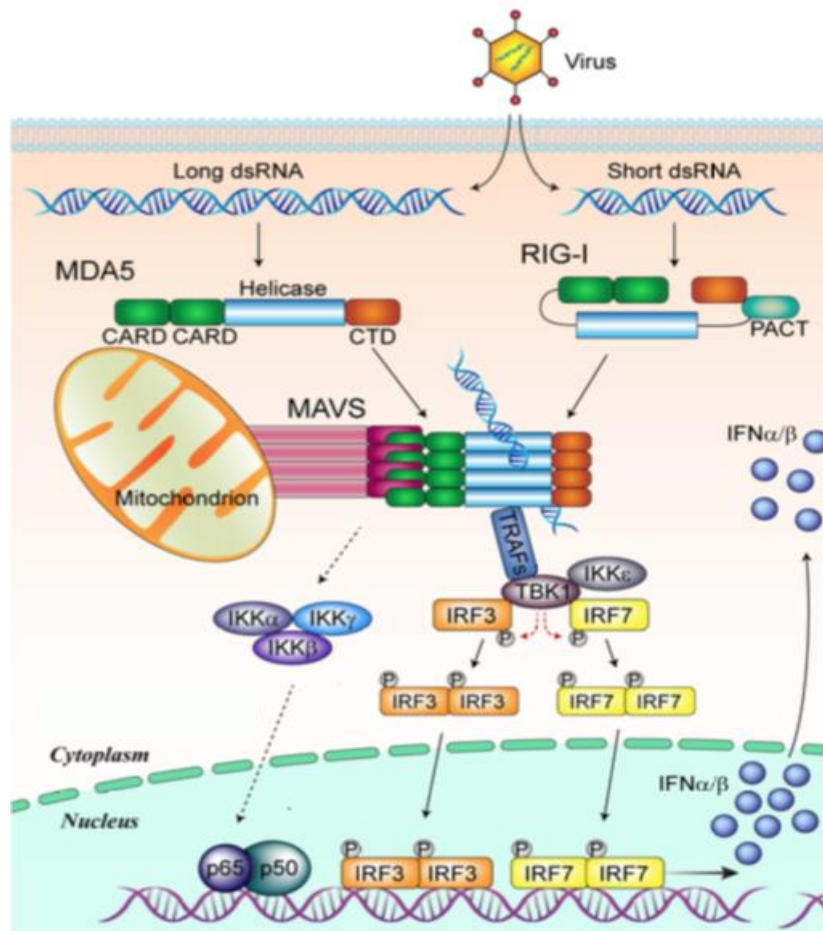
Figure 3. An overview of the Rig-I and MDA5 signaling pathways activated by a virus infection. P is a symbol for phosphate. Modified from Jin et al. (2017).

Rig-I, like MDA5, have caspase recruitment domains (CARDs) in the N-terminus of the protein, and in C-terminus an RNA helicase domain (DExD/H box helicase), which can bind and unwind dsRNA by an ATPase function (Yoneyama et al. 2004; Yoneyama et al. 2005; Saito et al. 2007; Takahasi et al. 2008). The CARD domains of Rig-I and MDA5 are responsible of mediating the signal downstream via the CARD domains of MAVS (Yoneyama et al. 2005; Saito et al. 2007; Loo et al. 2008). The nuclear Rig-I functions independently of MAVS (Liu et al. 2018). Rig- I is found as a monomer in uninfected cells (Saito et al. 2007). When the helicase domain of Rig-I binds it ligand and the ATPase function is active, the Rig-I undergoes multimerization and conformational change achieving active state (Saito et al. 2007; Takahasi et al. 2008). This is thought to be tightly regulated by a repressor domain (RD) in the C-terminus of the Rig-I (Saito et al. 2007).

Rig-I can recognize short dsRNA structures and RNAs with 5′-triphosphate ends, which may be present in virus infected cells either as incoming material

or as products of the viral RNA processing (Yoneyama et al. 2004; Hornung et al. 2006; Baum et al. 2010). On the other hand, MDA5 functions in recognizing mainly long dsRNA structures, like those present in picornaviruses (Kato et al. 2006; Jiang et al. 2011; Feng et al. 2012). Therefore, the activation of MDA5 and Rig-I is clearly distinctive. In transfection experiments by Jiang et al. (2011) human monocytic dendritic cells (moDCs) were transfected with synthetic RNAs of different length and properties (ss and ds and 5'- phosphorylated or 5'- dephosphorylated). In this study, they found that 5' phosphorylation of the short ssRNAs (58, 88 and 108 nt) was basically necessity for the IFN (IFN-α1, IFN-β, IFN-λ1) induction process (Jiang et al. 2011). On the contrary, 5' phosphorylation of the short dsRNAs (58, 88 and 108 nt) had a significant suppressive effect to the IFN (IFN-α1, IFN-β, IFN-λ1) induction process (Jiang et al. 2011). On the other hand, long ssRNAs (708 and 1808 nt) that were 5'-dephosphorylated were able to induce the production of those IFNs (Jiang et al. 2011). Jiang et al. (2011) also found that ssRNA was altogether weaker activator of the Rig-I pathway than short dsRNA. Moreover, they concluded that the Rig-I mediated IFN expression was more sensitive to the size variation of dsRNA than ssRNA (Jiang et al. 2011). To conclude, they found that short dsRNAs were the most efficient in the capacity to activate Rig-I mediated pathway (Jiang et al. 2011). Additionally, they found that the origin of the virus sequence was unimportant in the activation process of dendritic cells (DCs) (Jiang et al. 2011).

Schlee et al. (2009) studied more the requirements of Rig-I ligands. They found that synthetic 5' triphosphate single-stranded RNA was insufficient to activate Rig-I and IFN production. A rather short, around 20 bp long, blunt-end (panhandle) double-strand RNA with a 5' triphosphate end was the most favorable to activate Rig-I (Schlee et al. 2009). Such molecules are seen in panhandle structures of single-stranded RNA virus genomes (Schlee et al. 2009). Schlee et al. (2009) also showed that minor mismatches and bulge loops of the panhandle structure, which might occur in negative-sense RNA viruses, are tolerated, i.e. the structure is still recognized by Rig-I. This supports the idea that Rig-I recognition relies only on double-stranded RNA structures. To add more discrepancy, Choi et al. (2009) have found that Rig-I functions as a cytosolic dsDNA sensor as well. Conclusively, like proven by multiple different studies presented above, the activation of the Rig-I pathway

is still somewhat unclear and studies with data from authentic infections are less common than transfection experiments.

Activated Rig-I recruits MAVS, which mediates the signal downstream (Kawai et al. 2005; Seth et al. 2005). Downstream in the signaling cascade is a TNF receptor associated factor (TRAF) protein, TRAF3, which interacts with MAVS and is proven to be crucial for IFN induction in SeV infection (Saha et al. 2006). To TRAF are associated TANK-binding kinase 1 (TBK1) and inhibitor of nuclear factor kappa-B kinase ε (IKKε), which are kinases responsible of phosphorylation and activation of interferon regulatory factor 3 (IRF3) (Fitzgerald et al. 2003; Sharma et al. 2003; McWhirter et al. 2004).

IRF3 is a transcription factor and binds to specific DNA regions and regulates interferon gene activation (Au et al. 1995; Juang et al. 1998; Sato et al. 1998; Yoneyama et al. 1998; Lin et al. 2000; Sato et al. 2000). IRF3 is expressed constitutively and widely in different tissues, and it locates in the cytosol (Au et al. 1995; Yoneyama et al. 1998). Like noted, IRF3 is activated by phosphorylation (Fitzgerald et al. 2003; Sharma et al. 2003; McWhirter et al. 2004) and it then undergoes dimerization (Sato et al. 1998; Yoneyama et al. 1998; Lin et al. 1999). Furthermore, the phosphorylated IRF3 dimer complex formation enables the complex to recruit its coactivator CBP/p300 complex (Sato et al. 1998; Yoneyama et al. 1998; Lin et al. 2000). This allows the translocation of the whole complex from cytosol into nucleus (Sato et al. 1998; Yoneyama et al. 1998; Lin et al. 2000).

In the nucleus IRF3/CBP/p300 complex induces the expression of antiviral genes such as type I IFNs like IFN-β (Sato et al.1998; Juang et al. 1998; Lin et al. 2000; Österlund et al. 2007) and type III IFNs like IFN-λ1 (Österlund et al. 2007). Moreover, IRF3-dependent IFNs can further stimulate interferon stimulated genes (ISGs), like interferon-induced protein with tetratricopeptide repeats 2 (Ifit2 or ISG54) and interferon-induced protein with tetratricopeptide repeats 1 (Ifit1 or ISG56) (Grandvaux et al. 2002; Loo et al. 2008), that in turn lead to production of other pro-inflammatory cytokines, which function in cell interactions and modulate immune responses (Fensterl and Sen 2009). An example of pro-inflammatory cytokines, which expressions are elevated and mediated by IRF3 are a protein called regulated on activation, normal T cell expressed and secreted (RANTES) (Lin et al. 1999; Génin et al. 2000; Fitzgerald et al. 2003) and C-

X-C motif chemokine 10 (CXCL10) (Brownell et al. 2014), which are chemokines that attracts immune cells to the infection site and activates them (Sokol and Luster 2015). In addition to the IFN and further chemokine production stimulus function, IRF3 has also been shown to form a complex with a pro-apoptotic Bax protein, which mediates apoptosis (Chattopadhyay et al. 2011). The activation of Rig-I and MDA5 also leads to the activation of a transcription factor Nf-kB (p50 and p56 forms the Nf-kB transcription factor complex Urban et al. 1991), which is able to mediate type I interferon production as well through TRAF6 (Yoneyama et al. 2004; Konno et al. 2009; Lee et al. 2015).

There is evidence that Rig-I is crucial for recognizing paramyxoviruses like SeV. Kato et al. (2005) showed that in mice lung fibroblasts (MEFs), Rig-I mediated activation of interferon production post SeV infection is pointed to be indispensable. Loo et al. (2008) came to the same conclusion, since they found that in SeV infection in MEFs, IRF3 translocation into nucleus was dependent on Rig-I (in Rig-I -/- MEFs the IRF3 translocation was totally absent). On the other hand, Kato et al. (2006) showed that while Rig-I is essential for SeV induced type I IFN production, in a picornavirus, encephalomyocarditis virus (EMCV), infection type I IFN production was not abolished in Rig-I deficient MEFs. In this study, they also got similar kind of results with human Rig-I in transfection experiments (Kato et al. 2006). Therefore, in the case of SeV-infection, the recognition of the virus and the mediation of antiviral responses by the Rig-I definitely seem to be of most importance. Altogether, these findings support the idea that, especially in the case of SeV infection, Rig-I pathway is the key mediator of the activation of IFN production via the activation of IRF3.

To conclude, activation of the Rig-I pathway after a virus infection leads to activation of IRF3 transcription factor, which in turn activates the production of interferons. The innate immunity responses vary between different cell types and viruses. Furthermore, IFNs activate interferon stimulated genes (ISGs), and this cascade is discussed more next.

## 1.5 Interferons (IFNs) and activation of interferon stimulated genes (ISGs)

Cytokines are proteins that function in cellular signaling processes (Takaoka and Yanai 2006). They are key mediators of immune responses and can

function as autocrine and / or paracrine meaning that they activate either the cell that produced them or the neighboring cells, respectively (Takaoka and Yanai 2006). One group of cytokines, interferons (IFNs), are especially important in virus infections, since they initiate the activation of antiviral responses (Müller et al. 1994; Hwang et al. 1995; Der et al. 1998; Takaoka and Yanai 2006). Specifically, Type I IFNs are of great importance in virus infections (Müller et al. 1994; Takaoka and Yanai 2006). The group of type I IFNs consist of -α, - β, and other minor groups, and alone 13 different subtypes of interferon α have been introduced (Takaoka and Yanai 2006; Fensterl and Sen 2009). IFN-γ represents type II IFNs (Takaoka and Yanai 2006) while type III interferons are a bigger group consisting of four IFN-λ subtypes (Kotenko et al. 2003; Prokunina-Olsson et al. 2013).

Once bound to their receptor on cell surface, IFNs elicit pleiotropic downstream effects on the host cell and its viability, such as inhibition of proliferation, regulation of apoptosis, and acting as immunomodulators (Der et al. 1998). For instance, Ngyuen et al. (2002) demonstrated in murine cytomegalovirus (MCMV) infected mice that NK cells and their cytotoxic effect towards infected cells are activated and regulated by IFN-$\alpha\beta$ cytokines and downstream signaling molecules activated by these cytokines. As seen in figure 4, human IFN α/β receptor is a transmembrane (single loop), dimeric receptor, and can bind type I IFNs (Novick et al. 1994).
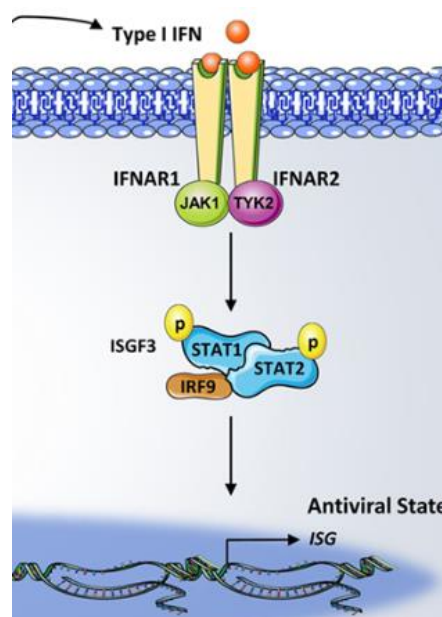


Figure 4. The structure of human interferon α/β receptor and its simplified signaling pathway in response to type I interferons. Modified from Cox and Plemper (2015).

14

One of the subunits of the IFN α/β receptor is directly linked to tyrosine kinase JAK1 in one of its cytoplasmic subunits (Novick et al. 1994) (Figure 4). Additionally, a tyrosine kinase (Tyk2) has been shown to be associated with the receptor in the cytoplasmic part of the other subunit (Abramovich et al. 1994). IFN-λ mediates signal via type II cytokine receptor complex forming of two subunits: IFN-λR and CRF2-4 (Kotenko et al. 2003). IFNs activate antiviral state principally via the Jak/STAT pathway, which then activate antiviral responses (Darnell et al. 1994).

Signal transducers and activators of transcription (STATs) are a group of signaling molecules that are activated by tyrosine phosphorylation by IFNs (Darnell et al. 1994). Janus protein tyrosine kinases (Jaks) are responsible of the phosphorylation of STATs (Darnell et al. 1994). Therefore, specific IFNs can act as ligands for Janus protein tyrosine kinase (Jak) receptors, and Jaks further activate STATs (Darnell et al. 1994). Once Jak has bound its ligand, it is phosphorylated and then two STAT molecules bind to it (Darnell et al. 1994). In the case of some Type I IFNs, these are STAT1 and STAT2, which are then phosphorylated and form a dimer (Shuai et al. 1994; Meraz et al. 1996; Park et al. 2000) and to this complex, interferon regulatory factor 9 (IRF9) is further bind (Veals et al. 1992; Veals et al. 1993). This complex of three polypeptides is referred as interferon-stimulated gene factor 3 (ISGF3) (Schindler et al. 1992; Veals et al. 1992; Müller et al. 1993; Veals et al. 1993). The ISGF3 complex can then enter into the nucleus, and specifically IRF9 binds to interferon-stimulated response element (ISRE), and thus function as a transcription factor (Veals et al. 1992; Veals et al. 1993; Shuai et al.1994) and regulate bunch of interferon stimulated genes (ISGs) (Li et al. 2017).

These ISGs, such as *ISG54*, *ISG56*, *2-5A - dependent RNase L* genes, *dsRNA-activated protein kinase* (PKR) gene, and *MxA* genes, are related to cell survival, proliferation, inhibition of virus replication, immune cell activation (NK cells), and recruitment (Pavlovic et al. 1990; Müller et al. 1994; Der et al. 1997; Zhou et al. 1997; Der et al. 1998; Ngyuen et al. 2002; Fensterl and Sen 2009). Similar to type I IFNs, the type III IFN signaling pathway includes phosphorylation of STAT1 and STAT2 followed by activation of ISGF3 complex and expression of ISGs (Kotenko et al. 2003; Prokunina-

Olsson et al. 2013). Taken this all together, innate immunity and IFN signaling is highly complex and much is still unknown.

## 1.6 Strategies of paramyxoviruses to evade antiviral responses

Viruses have evolved means to inhibit the activation of antiviral responses in order to ensure their propagation in the host cell. SeV C and V proteins have been found to inhibit pathway leading to the activation of IRF3, thus inhibiting the activation of interferon, such as interferon-$\beta$, production and therefore activation of interferon stimulated genes (ISGs) and consequently antiviral responses (Poole et al. 2002; Andrejeva et al. 2004; Komatsu et al. 2004; Irie et al. 2012). SeV V protein has been shown to bind and inhibit MDA5 but on the other hand it is incapable to interact with and inhibit RIG-I receptors in mammal and avian cells (Childs et al. 2007). Another immuno-evasion strategy of viruses is the ability to prevent apoptosis, which was mentioned earlier regarding SeV C proteins (Koyama et al. 2003).

## 1.7 Aims of this study

The early points of SeV infection and the mechanisms of the Rig-I pathway activation are unclear. The aim of this project was to study the first hours of SeV infection in cell culture conditions and the effects regarding the activation of antiviral responses by the Rig-I signaling pathway. Additionally, one central question was whether the virus needs to replicate in order to be recognized by the Rig-I or if it is enough that the virus just enters the cell. More specifically, this study concentrated on the activation and localization kinetics of IRF3 protein as well as initiation of *IFN-$\beta$1*, *IFN-$\lambda$1*, and viral N protein encoding mRNA expression following SeV infection in lung epithelial cells. The expression of viral proteins as well as host IRF3 protein after the infection were also examined.

# 2. Materials and Methods

## 2.1 Cells and the virus

Human adenocarcinomic lung epithelial cells, A549 cells, were used in the experiments, since sendai virus infects primarily bronchial epithelial cells (Ishida and Homma 1978). The cells were cultured in T75-flasks using RT-

warmed (approximately + 25 °C) growth medium (Attachment 1). All the used mediums were RT-warmed prior use unless otherwise noted. Cells were grown in 5 % $CO_2$ conditions at + 37 °C. The protocol for detaching adherent A549 cells is in attachments (Attachment 2). For fixing, the cells were washed with Phosphate-buffered saline (PBS), and 3 % paraformaldehyde (PFA) in PBS was then added. The cells were incubated for 15 min and then washed twice with PBS and stored in PBS at + 4 °C and further analyzed within approximately two days.

The sendai virus stock used, strain Cantell, has been prepared (2014 by Julkunen group) from viruses grown in chicken eggs and stored in - 80 °C. The early history of the Cantell strain is vague, but it has been first used in Finnish Institute for Health and Welfare (former Central Public Health Institute) Laboratory in Helsinki (Cantell et al. 1981; Cantell and Hirvonen 1981). It is distributed for example by American Type Culture Collection (ATCC) that came up with the name Cantell strain (ATCC® VR-907™). The strain induces efficiently interferon production (Cantell et al. 1981; Cantell and Hirvonen 1981), which makes it suitable for this study.

## 2.2 Determining the Multiplicity of Infection (MOI) of SeV in A549 cells

The Multiplicity of Infection (MOI) was determined with plaque forming unit (PFU) assay and with focus forming unit (FFU) assay. In FFU assay, A549 cells were seeded onto a 96-well plate ($1,5x10^4$ cell / well, total volume 200 µl / well) in growth medium and let to attach to the plate surface in 5 % $CO_2$ conditions at + 37 °C overnight. The plate was examined with microscope to confirm the cell growth (> 80 %), and the cells were infected with different dilutions ($10_{-1}$ – $10_{-10}$) of SeV in HAM's F12 medium (Cytiva) (Attachment 3) with 1 % Fetal Bovine Serum (FBS) and 10 µg / ml of gentamycin sulphate (Biological Industries). The plate was incubated in 5 % $CO_2$ conditions at + 37 °C overnight. The cells were fixed (chapter 2.1). The immunofluorescent staining was done with 1:250 dilution of primary anti-SeV (rabbit anti-SeV polyclonal K2350 1991) followed with 1:200 dilution of secondary antibody (Alexa Fluor 488, goat anti-rabbit IgG, Invitrogen). The plate was analyzed with EVOS FL Auto Imaging System (Invitrogen) microscope, and colored foci were enumerated. The formula to calculate the titer (FFU / ml) was following:

$$\text{Focus Forming unit / ml (FFU / ml)} = \frac{number\ of\ viral\ foci}{dilution\ x\ volume\ of\ virus\ added\ to\ the\ well}$$

.

The desired MOI values for the experiments were then calculated with following formula:

$$V_{\text{virus-stock}} = \frac{desired\ MOI\ value\ x\ number\ of\ cells}{FFU/ml}$$

.

In PFU assay, the cells were seeded onto a 96-well plate ($1,5 \times 10^4$ cell / well, total volume 100 µl / well) in HAM's F12 medium with 1 % FBS and 10 µg / ml of gentamycin sulphate and let to attach to the plate surface in 5 % $CO_2$ conditions at + 37 °C overnight. The cells were infected with different dilutions ($10^{-1} - 10^{-10}$) of SeV in infection medium (OPTIMEM 1x Reduced serum medium, Life Technologies) and incubated in 5 % $CO_2$ conditions at + 37 °C for one hour. The medium along with the virus suspension was replaced with 1x DMEM medium (Lonza) (Attachment 4) supplemented with 1 % FBS, 10 µg / ml of gentamycin sulphate, and AVICEL (1,2 %, FMC BioPolymer). The incubation was continued in 5 % $CO_2$ conditions at + 37 °C for three days. The AVICEL overlay was aspirated and the cells were fixed (chapter 2.1). The fixed cells were washed with PBS twice and stained with crystal violet (100 µl / well), a DNA stain, for 20 min and washed twice with water. The plate was analyzed with EVOS FL Auto Imaging System (Invitrogen) microscope to count the plaques. The formulas to calculate the titer (PFU / ml) was following:

$$\text{Plaque Forming unit / ml (PFU / ml)} = \frac{number\ of\ plaques}{dilution\ x\ volume\ of\ virus\ added\ to\ the\ well}$$

.

The desired MOI values for the experiments were then calculated with the following formula:

$$V_{\text{virus-stock}} = \frac{desired\ MOI\ value\ x\ number\ of\ cells}{PFU/ml}$$

.

## 2.3 Immunocytochemical staining

Sterilized coverslips made of glass were placed on the bottoms of the wells of two 24 well plates. The cells were seeded onto the coverslips on the two 24 well plates ($5 \times 10^4$ cells / well) using growth medium (400 µl / well) and incubated in 5 % $CO_2$ conditions at + 37 °C overnight. The cells were infected with SeV at a MOI of 3700 (plate one) or 60 (plate two) in 200 µl of infection medium per well in 5 % $CO_2$ conditions at + 37 °C for an hour. The infection medium was replaced to HAM's F12 with 1 % FBS and 10 µg / ml of gentamycin sulphate, and the cells were incubated in 5 % $CO_2$ conditions at + 37 °C. After different periods of time (15 min, 30 min, 1h, 2h or 4h) the cells were fixed (chapter 2.1).

Separate droplets (50 µl) of permeabilization-blocking -solution (PB-solution; 0,1 % Triton X-100, 1 % Bovine Serum Albumin (BSA), in PBS) were added onto a sheet of parafilm (Bemis). The coverslips were gently lifted from the 24 well plates with a curled sterilized needle, and each coverslip was placed onto a PB-solution droplet on the parafilm sheet. The coverslips were always placed so that the side of the coverslip to which the cells were attached was facing towards the solution droplet. The coverslips were incubated at RT for 30 min. The coverslips were transferred onto separate droplets (50 µl) of 1:100 diluted primary antibody anti-IRF3 (rabbit anti-IRF3 polyclonal KCVD8, produced in National Public Health Institute Laboratory by Österlund et al. 2005) or primary antibody anti-SeV (rabbit anti-SeV polyclonal K2330 1991) in PB-solution on parafilm sheet. They were incubated at RT for one hour. They were washed three times with PB-solution (on separate droplets (50 µl) on parafilm sheet). The coverslips were transferred onto separate droplets (50 µl) of 1:200 diluted secondary antibody (for anti-IRF3 Alexa Fluor 568, goat anti-rabbit IgG, Invitrogen and for anti-SeV Alexa Fluor 488, goat anti-rabbit IgG, Invitrogen) in PB-solution on parafilm sheet and incubated at RT covered from light for 30 min. The coverslips were transferred onto separate droplets (50 µl) of 0,01 % Triton-X100 in PBS solution on parafilm sheet and incubated at RT for 10 min. The coverslips were washed three times for five min with PBS (on separate droplets (50 µl) on parafilm sheet).

The stained coverslips were mounted with an antifade-solution (ProLong Gold antifade reagent with 4′,6-diamidino-2-phenylindole (DAPI), Life technologies) on microscope slides and imaged shortly after with Leica fluorescent microscope (Leica DFC7000 T 2.8 MP Color Microscope Camera) and Las X software. If not imaged shortly after mounting, the slides were stored at + 4 °C, and covered from light, and used within approximately two days.

## 2.4 Immunocytochemical staining with cycloheximide (CHX)

The cells on coverslips were prepared like described in chapter 2.3 (two 24-well plates, 6 x 10$^4$ cells / well, total medium volume 450 µl / well). The next day, the plates were checked with microscope to confirm the cell growth (> 70 %). In the cycloheximide (CHX) treated plate, the growth medium was replaced with infection medium containing 10 µg / ml of CHX (Sigma-Aldrich) and incubated in 5 % $CO_2$ conditions at + 37 °C for 30 min. The cells on the CHX treated (CHX+) and CHX untreated (CHX-) plates were infected at a SeV MOI of 3700 (total volume 100 µl / well) in infection medium containing CHX (10 µg / ml) or without CHX, respectively, in 5 % $CO_2$ conditions at + 37 °C for an hour. The infection medium was replaced to HAM's F12 with 1 % FBS and 10 µg / ml of gentamycin sulphate, and the cells were incubated in 5 % $CO_2$ conditions at + 37 °C. The cells were fixed at different periods of time (15 min, 30 min, 1h, 2h or 4h) (chapter 2.1). The protocol for coverslips staining against anti-IRF3 (rabbit anti-IRF3 polyclonal KCVD8, produced in National Public Health Institute Laboratory by Österlund et al. 2005) was the same as described in chapter 2.3. The stained coverslips were mounted, imaged, and stored like described in chapter 2.3.

## 2.5 Protein expression by immunoblotting

A549 cells were seeded onto 6-well plates (5x10$^5$ cells / well; 2,5 ml medium per well) in growth medium and let to attach in 5 % $CO_2$ conditions at + 37 °C overnight. The cell growth was examined (> 80%) and the cells were infected with SeV at a MOI 180 in infection medium in 5 % $CO_2$ conditions at + 37 °C for an hour. The infection medium was replaced to HAM's F12 with 1 % FBS and 10 µg / ml of gentamycin sulphate and the cells were incubated in 5 % $CO_2$ conditions at + 37 °C.

The cells were lysed in different time points after the infection (2h, 4h, 6h, 8h, 16h and 24h) with 300 µl of ice-cold lysis buffer (100 mM Tris-HCl, pH 7.5, 150 mM NaCl, 1x Passive Lysis buffer (Promega), 1x PhosphoStop (Roche), 25 % ethylene glycol, 1 x c0mplete (C0mplete Tablets, Mini EDTA-free, EASYpack, Roche); 0,1 % Benzonase nuclease (Sigma)). The lysing was performed on ice. The lysates were collected into separate Eppendorf tubes and the wells were examined to be empty of cells with microscope. The lysates were stored at - 20 °C until further analysis within two days.

Total protein concentrations of the collected lysates were measured with detergent compatible Bradford assay (Pierce™ Detergent Compatible Bradford Assay kit, Thermo Scientific) in a 96-well plate. The albumin standards were diluted according to the bigger working range (100 - 1500 µg / ml) according to the instructions of the Bradford assay manufacturer. The microplate protocol for the measurements was done according to the manufacturer's instructions. Absorbance of the standard replicates and of each unknown sample was measured at 595 nm with a plate reader (Multimode Plate Reader, Victor Nivo, PerkinElmer). From the gotten standard values, average absorbance of each sample was calculated and from those, a standard curve was constructed. For each unknown sample, an average absorbance was calculated, and protein concentration was determined from the standard curve.

Twenty µg of protein per sample was used in sodium dodecyl sulfate polyacrylamide gel electrophoresis (SDS-PAGE) run. The samples were diluted with 2x SDS loading detergent (4 % SDS, 10 % β-mercaptoethanol, 30 % glycerol in 0,5 mM of Tris-HCl, pH 8) in 1:2. The samples were boiled in Eppendorf tubes at + 98 °C for 5 min. The samples were cooled down to RT and mixed before loading in the wells of the PAGE-gels (Mini-PROTEAN TGX™ gels, Bio-Rad). Pre-stained protein ladder (Chameleon™ Duo Pre-stained Protein Ladder, LI-COR) (five µl) was used in one well of each gel. SDS-PAGE run was performed at 200 V in 1x running buffer diluted in MQ (Bio-Rad 10x TGS buffer: 25 mM Tris, 192 mM Glycine; 0,1 % SDS, pH 8,3) for 35 min.

The SDS-PAGE gels were soaked in transfer buffer (25 mM Tris-HCl, pH 8,3; 192 mM glycine, 20 % (v/v) methanol) for two min. Two filter papers (Bio-Rad, Extra thick blot paper) and a nitrocellulose membrane (Whatman

Protran, pure nitrocellulose transfer and immobilization membrane) per gel were soaked in transfer buffer for 10 min. They were arranged in a semi-dry apparatus (Bio-Rad Trans-blot SD Semi-dry transfer cell) in following order: filter paper - membrane - gel - filter paper. Transfer was done at 13 V for 40 min.

The membranes were blocked with 5 % skimmed milk powder (Valio, Finland) in TBST (Tris buffered saline with 0,05 % Tween-20; pH 7,2 - 7,4) at RT for an hour. The membranes were washed with TBST for 5 min three times. The membranes were incubated with 1:250 of primary antibodies anti-IRF3 (rabbit anti-IRF3 KCU28 Ag/97/THL) and anti- glyceraldehyde 3-phosphate dehydrogenase (glyceraldehyde 3-phosphate dehydrogenase (GAPDH) mouse monoclonal 6C5 sc-32233, Santa Cruz) or anti SeV (rabbit anti-SeV polyclonal K2350 1991) that were diluted in 2,5 % blocking buffer in TBST in a shaker at RT for one hour. The membranes were washed with TBST for 5 min three times. The membranes were incubated with 1:15 000 dilution of secondary antibody (for anti-IRF3 and anti-SeV: goat anti-rabbit, IR dye 800CW, LI-COR and for GAPDH goat anti-mouse, IR dye 680RD, LI-COR) in 2,5 % blocking buffer on a shaker, covered from light at RT for 30 min. The membranes were covered from light, washed with TBST for 5 min three times, and imaged by Odyssey imaging system (Odyssey Fc, LI-COR) at corresponding wavelengths (680 nm and 800 nm) to the used secondary antibodies.

## 2.6 mRNA expression by quantitative reverse transcription PCR (qRT-PCR)

A549 cells were seeded onto 6-well plates ($5 \times 10^5$ cells / well; 2,5 ml medium / well) in growth medium in 5 % $CO_2$ conditions at + 37 °C overnight. The cells were infected with SeV at a MOI 5 or MOI 50 in infection medium in 5 % $CO_2$ conditions at + 37 °C for an hour. The infection medium was replaced to HAM's F12 with 1 % FBS and 10 µg / ml of gentamycin sulphate and the cells were incubated in 5 % $CO_2$ conditions at + 37 °C. At different time points (30 min, 1h, 2h, 4h, 8h, 16h and 24h) the cells were lysed (300 µl / well) with ice cold TRIzol reagent (TRIzol RNA Isolation Reagent, Invitrogen) that contains an RNase inhibitor. Each time point sample was collected from individual well and the lysing was performed on ice. The lysates were collected in Eppendorf tubes and stored at - 20 °C until further analysis within two days.

Total RNA in the samples was extracted by chloroform-isopropanol extraction method, since RNA yield, purity, and accuracy of RNA quantification by qRT-PCR have been demonstrated to be good with that method (Toni et al. 2018). 100 µl of chloroform was added to each sample and shook well by hand for 15 seconds after which the samples were let to sit at RT for 3 min. The samples were centrifuged at 12 000 x g, 15 min, at + 4 °C. The upper aqueous layers were carefully collected into new RNase free Eppendorf tubes that had 100 µl of chloroform in them. The tubes were shaken well by hand for 15 seconds and let to sit at RT for 3 min. The samples were centrifuged at 12 000 x g, 15 min, at + 4 °C and the aqueous layers were transferred into new tubes containing 250 µl of isopropanol to precipitate the RNA. The tubes were inverted by hand for approximately 15 times and let to sit at RT for 10 min. The samples were centrifuged at 12 000 x g, 10 min, at + 4 °C. The supernatants were gently poured and discarded, and the pellets were washed with 1 ml of 75 % EtOH in MQ and centrifuged at 7500 x g, 5 min, at + 4 °C. The supernatants were poured out and discarded and this washing with 1 ml of 75 % EtOH in MQ was repeated two more times. The remaining pellets were pulse spinned at RT and the remaining supernatants were carefully removed with pipet and the tubes were left open for 5 min. The tubes were heated in a heat block at 65 °C for 5 min.

The RNAs were solubilized to 20 µl of RNase free water (Thermo Fisher scientific) and heated at 65 °C for 5 min. The samples were mixed briefly and spinned and the RNA concentration and quality were determined with spectrophotometer measuring the absorbance in 260 nm as well as the 260/230 and 260/280 ratios of each sample (DeNovix, DS- 11+ Spectrophotometer). One µl of each sample was mixed by pipetting and then pipetted on the detector. Concentration results are in ng / µl. The RNA samples were stored at - 80 °C until further analysis within two days.

The purified RNA samples were transcribed into cDNA in reverse transcription (RT) reaction (1 µg of RNA sample / reaction) with a reverse transcriptase (1x RT Buffer; 500 µM dNTPs; 1 µM random Hexamers; 0,4 U / µl Rnase inhibitor, 200 U / µl RevertAid H minus reverse transcriptase all from Thermo Scientific). The RT reaction was carried out in a thermal cycler (MJ Research, PTC-200 Peltier Thermal Cycler) and with RevertAid RT

program (Hold at 25 °C for 10 min, hold at 42 °C for 60 min and hold at 70 °C for 10 min). The cDNA samples were stored at - 20 °C until further analysis within two days.

CDNA samples were run in qPCR reaction. In the reaction, 2,5 µl of cDNA sample (50 ng) was added in 17,5 µl of PCR mix (1x TaqMan™ Universal PCR Master Mix, 1x TaqMan™ Gene Expression Assay, nuclease-free water all from Thermo Fisher scientific) in a PCR tube, mixed briefly and ran on PCR machine (Rotor-Gene Q, Qiagen). The primers used to detect specifically SeV N protein encoding sequence were designed in-house. The specific primers and Taqman™ FAM-labeled probe for SeV N protein encoding sequence were: SeV N-sense (5'-CCAACCCCACCGACCACAC-3'), SeV N-antisense (5'-GAATCCGATAACATCCGAGAGCGAC-3') and SeV N-FAM-probe (6'- fluorescein amidite (FAM)-TCGAGACAGCCACGGCTTCGGCTAC-BHQ1'). For *IFN-β1* (1x mix Hs00277188_s1 IFNB1, Thermo Fisher scientific) and for *IFN-λ1* (1x mix Hs00601677_g1 IFNL1, Thermo Fisher scientific) were used. The setup for the amplification reaction was following: Hold at 50 °C (2 min), hold at 95 °C (10 min), 40 cycles of two steps that were first (step 1) hold at 95 °C (15 s) followed with (step 2) hold at 60 °C (60 s).

The data was processed with the Rotor-Gene Q Software 2.3.1.49. The threshold for the fluorescence signal, Cyclin A (Green), was set so that it cropped low or unspecific signal curves out. The noise slope correction and dynamic tubes normalization were done with the software. The raw data (Cycles to Threshold -values, $C_T$-values) were further analyzed with $\Delta\Delta C_T$-method. The result is given by $2^{-\Delta\Delta C_T}$, which represents the fold change in the expression of a gene in relation to a calibrator. The standard errors, which is obtained by dividing standard deviation by the square root of the total number of samples, of the results were calculated with excel.

## 2.7 mRNA expression of cells treated with CHX by qRT-PCR

A549 cells were seeded onto 6-well plates ($5x10^5$ cells / well; 2,5 ml medium / well) in growth medium in 5 % $CO_2$ conditions at + 37 °C overnight. The medium was replaced with infection medium containing 10 µg / ml of CHX (Sigma-Aldrich) and incubated in 5 % $CO_2$ conditions at + 37 °C for 30 min. The cells were infected with SeV at a MOI 1 in infection medium containing

10 µg / ml of CHX (Sigma-Aldrich) in 5 % $CO_2$ conditions at + 37 °C for an hour. The medium was replaced to HAM's F12 with 1 % FBS and 10 µg / ml of gentamycin sulphate and the cells were incubated in 5 % $CO_2$ conditions at + 37 °C. The cells were lysed at different time points after the infection as described in chapter 2.6. The total RNAs were extracted (chapter 2.6) and RT-reaction performed for them (chapter 2.6). CDNA samples were run in qPCR reaction with specific primers for SeV N protein encoding sequence, *IFN-β1*, and *IFN-λ1* (chapter 2.6).

# 3. Results

In this study the activation kinetics of the Rig-I pathway after sendai virus infection in A549 cells was examined and characterized. In addition, the activation requirements of the Rig-I pathway after the infection was studied. More specifically, a key interest was whether the Rig-I pathway is activated once the virus is in the host cell or once the virus is replicating. These research questions were approached by studying the kinetics and the movement of the transcription factor IRF3 after the infection. In addition, host and viral protein expressions after the infection were studied. Additionally, the activation of *IFN-β1*, *IFN-λ1*, and viral N protein encoding mRNA expressions after the infection were studied.

Three different methods were used for the studies: immunocytochemical staining, immunoblotting, and qRT-PCR. The immunocytochemical staining experiments were done with cells that were either treated or untreated with CHX before and during the SeV infection. With these experiments it was possible to study the localization of IRF3 in the presence or absence of protein synthesis in SeV-infected cells. Therefore, the activation requirements of the Rig-I pathway could be studied. IRF3 and viral protein expression kinetics were studied by immunoblotting. To study host (*IFN-β1* and *IFN-λ1*) and viral (N protein encoding) mRNA expression kinetics, qRT-PCR was performed with both CHX treated and untreated cells.

## 3.1 Determination of SeV stock titer

Virus stock titers can be estimated with Plaque Formin Unit (PFU) and Focus Forming Unit (FFU) assays. With the stock titer value, the desired MOI value

of an infection experiment can be assessed. In the PFU assay, the virus titer is calculated on the basis of the plaques, i.e. holes, formed on the cell layer due to cell death after the infection. With the FFU assay, the virus titer is calculated on the basis of the number of dye focus points when the infected cells are stained with the virus specific antibody. These two assays were used to determine the SeV stock titer.

In the PFU assay the cells were infected with a serial dilution ($10^{-1}$ – $10^{-10}$) of SeV and MOCK cells were uninfected. Four replicates of each used dilutions were made. The virus suspension was changed into medium that contained 1 % FBS as well as 1,2 % AVICEL after an hour. The cells were incubated for three days. The AVICEL overlay was aspired, the cells were fixed, and stained with crystal violet to visualize the formed holes in the cell layer with a microscope. The cell layers in each used dilution of SeV, as well as in MOCK wells, were excessively detached from the bottom of the wells (data not shown). Therefore, this method was incapable to determine the SeV stock titer value.

Instead, the calculations were done based on the FFU assay. In the FFU assay the cells were infected with a serial dilution ($10^{-1}$ – $10^{-10}$) of SeV and MOCK cells were uninfected. Three replicates of each used dilutions were made. The cells were incubated overnight, fixed, and stained with polyclonal anti-SeV antibody. The formed dye focus points were calculated with a microscope. Adequate number of dye spots (foci) for the calculations were in wells infected with $10^9$ dilution of SeV. Hence, this dilution was chosen from which the FFU / ml was determined. From the four replicate wells of the $10^9$ dilution, an average number of foci was first calculated. Then the FFU / ml value was determined with the formula described in the methods. An estimation of $6 \times 10^9$ FFU / ml for the A549 cells was obtained. This shows that the SeV stock used in the experiments was viable and potent. Based on the FFU / ml value, the MOI value of infection experiments, i.e. how much virus stock was necessary to add to the cells ($V_{virus-stock}$) to obtain desired MOI, could be determined with the second formula described in the methods.

## 3.2 Visualizing translocation kinetics of IRF3 into nucleus after SeV infection

Activation followed by translocation of IRF3 from cytoplasm into the nucleus is a signal that innate immunity pathways are activated, since IRF3 is

downstream of important PRRs functioning in virus infections. Location of IRF3 in the cell and its potential translocation into the nucleus after SeV-infection was studied with immunocytochemical staining of the infected cells. The cells were infected with a MOI of 3700 and MOCK cells were uninfected. The cells were fixed at different time points (15min, 30min, 1h, 2h, or 4h) after the infection, stained with polyclonal anti-IRF3, and imaged with fluorescent microscope. In uninfected A549-cells the nucleus of the cells appeared darker than the surrounding cytoplasm (Figure 5. A).
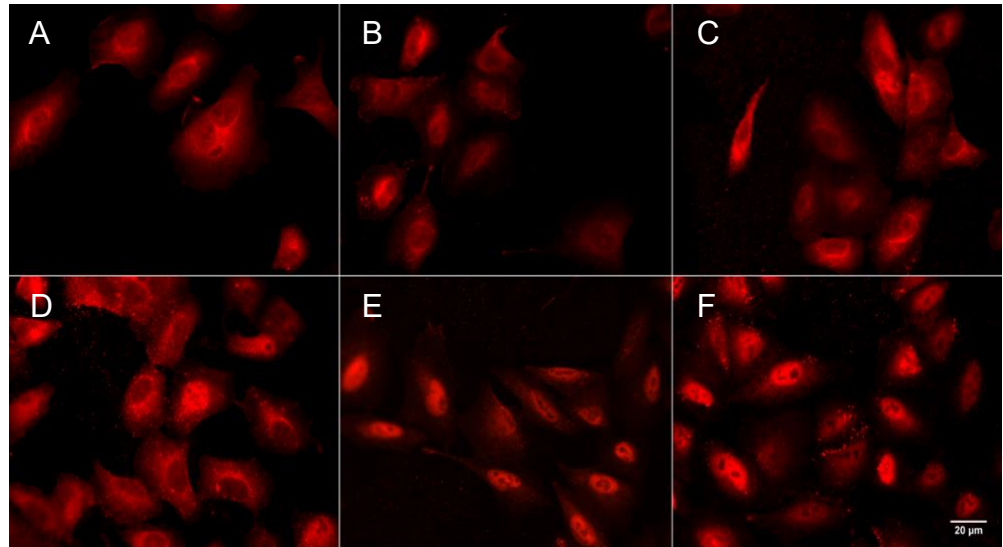


Figure 5. SeV infection triggers early translocation of IRF3 into the nucleus. Anti-IRF3 stained (in red), SeV (MOI 3700) infected A549 cells. A) MOCK cells. The cells were fixed at B) 15min, C) 30min, D) 1h, E) 2h or F) 4h after the infection and imaged with Leica fluorescent microscope with 63x zoom. The scale bar (20 µm) of all images is shown in the far right.

Therefore, IRF3 located in the cytoplasm in uninfected cells. The nucleuses appeared darker than the surrounding cytoplasm also 15 min and 30 min after SeV-infection (Figure 5. B and C). Consequently, IRF3 located in the cytoplasm in those as well. However, one hour after the infection, some cells had bright red nucleuses (Figure 5. D). This indicates that IRF3 was in nucleus already one hour after infection. The number of cells that had bright red nucleuses, hence, IRF3 located in the nucleus, increased remarkably as the infection progressed, i.e. four hours after the infection virtually every nucleus had concentrated amount of IRF3 (Figure 5. D, E and F). To conclude the results, the IRF3 translocation into nucleus was observed as soon as one hour after the SeV-infection.

## 3.3 Visualizing translocation kinetics of IRF3 into the nucleus after SeV-infection when protein synthesis is blocked

Like stated previously, the activation of IRF3 results in its translocation from cytoplasm into the nucleus and this indicates that innate immunity PRRs have been activated. To study whether SeV needs to replicate in order to activate the translocation of IRF3 and therefore the activation of innate immunity PRR pathway functions, protein synthesis was blocked with CHX in this immunocytochemical staining experiment. The cells were treated with CHX before and during the infection at a MOI of 3700 (MOCK cells were uninfected). The cells were fixed at different time points and stained with polyclonal anti-IRF3 and imaged with fluorescent microscope. In the CHX+ MOCK cells the nucleuses appeared darker than the surrounding cytoplasm (Figure 6. A).
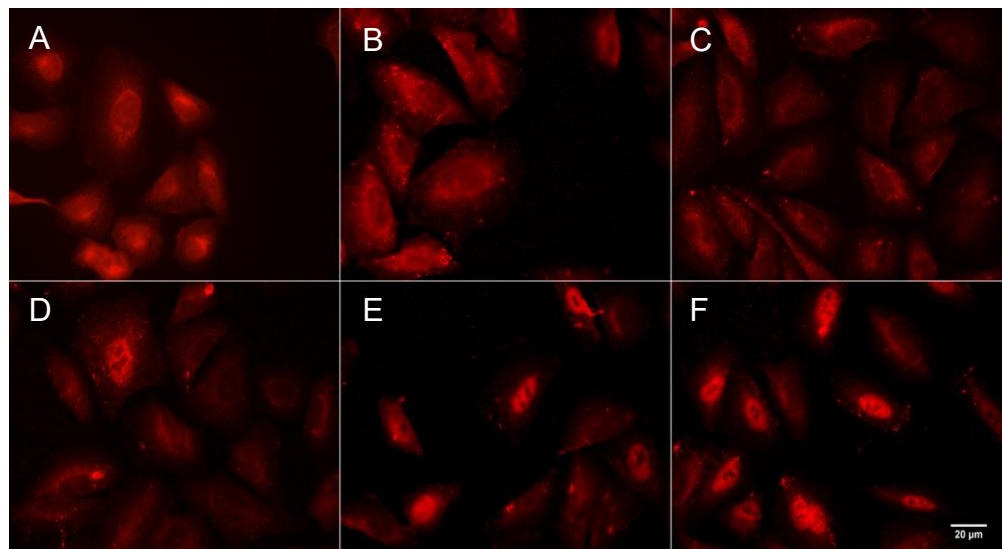


Figure 6. Blocking protein synthesis does not prevent IRF3 translocation into the nucleus. Anti-IRF3 stained (in red) SeV (MOI 3700) infected and CHX treatedA549 cells. A.) CHX+ MOCK cells. The cells were fixed at B.) 15min, C.) 30min, D.) 1h, E.) 2h or F.) 4h after the infection and imaged with Leica fluorescent microscope with 63x zoom. The scale bar (20 µm) of all images is shown in the far right.

This means that IRF3 located in the cytoplasm in MOCK cells. Likewise, the nucleuses appeared darker than the cytoplasm 15 min and 30 min after the infection in CHX+ cells (Figure 6. B and C). Hence, between that time, IRF3 was in the cytoplasm. Instead, one hour after the SeV-infection some of the nucleuses of the CHX+ cells were bright red (Figure 6. D). Therefore, by one hour after the infection, IRF3 was in the nucleus. From one hour onwards, majority of the cells had bright red nucleuses, which indicates that IRF3 was in the nucleus, and the number of cells having bright red nucleuses increased as the infection progressed (Figure 6. E and F). Consequently, the proportion

of cells having IRF3 in the nucleus increased as the infection progressed (Figure 6. E and F). In addition, fewer cells had bright red nucleuses, i.e. IRF3 located in the nucleus, two hours after SeV-infection in CHX+ cells when compared to corresponding time point of CHX- cells (Figure 5. E and Figure 6. E). To conclude, IRF3 translocated into the nucleus already one hour after the SeV-infection even when protein synthesis was blocked.

## 3.4 Visualizing the amount of SeV proteins in the cells after SeV-infection

When viruses have entered the host cell they start to replicate to produce progeny viruses. The accumulation kinetics of SeV proteins in cell cultures after SeV-infection was studied to see if and when the virus starts to accumulate and the location of the virus in the host cell. The cells were infected at a MOI of 60 (MOCK cells were uninfected), fixed at different time points, stained with polyclonal anti-SeV antibody, and imaged with fluorescent microscope. The results are seen in figure 7.
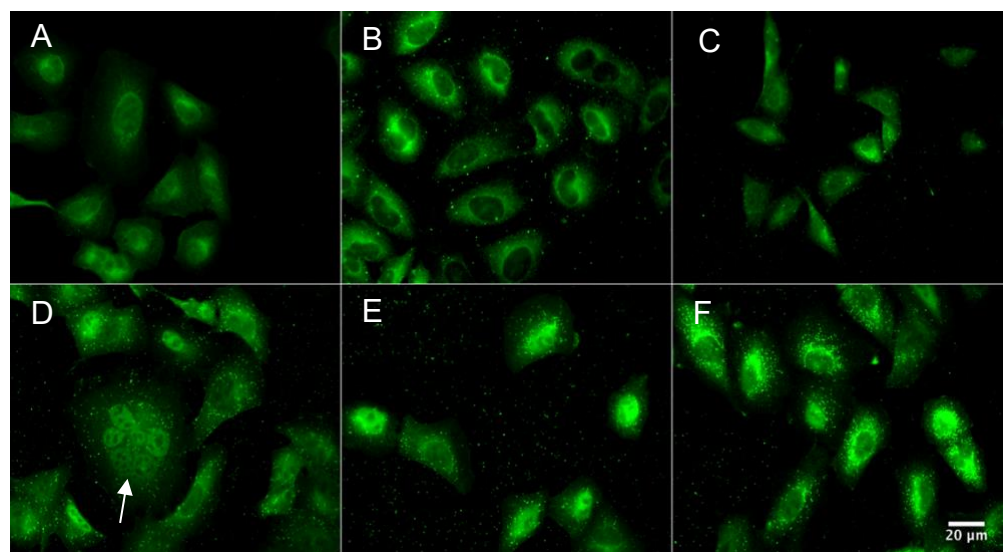
Figure 7. The amount of SeV around and in A549 cells is increasing as the SeV-infection progresses. Anti-SeV stained (in green) SeV (MOI 60) infected A549 cells. A.) MOCK cells. The cells were fixed at B.) 15min, C.) 30min, D.) 1h, E.) 2h or F.) 4h after the infection and imaged with Leica fluorescent microscope with 63x zoom. An arrow in picture D is pointing a possible polycaryocyte. The scale bar (20 µm) of all images is shown in the far right.

MOCK infected cells only had green background, so they lacked any bright green spots that indicate SeV proteins (Figure 7. A). Starting at 15 min after the infection, all the way to the last time point (four hours), bright green dye spots were visible (Figure 7. B, C, D, E, and F). Therefore, SeV proteins were present in those cells. In 15 min to 30 min after the infection, the bright green spots, which indicate SeV proteins, were scattered around the cells and

29

some were in the cells (figure 7. B, C). Instead, between one and four hours after the infection, the bright green spots, so the SeV proteins, were more concentrated in the cells and especially in the nucleus or the cytoplasm of the cells (figure 7. E, F). However, the most intense staining result occurred four hours after the infection (figure 7. F). The morphology of the cells that had bright green spots (SeV proteins) mostly located in the nucleus were rounder than those that them mostly in the cytoplasm (figure 7. E, F). In addition, a possible polycaryocyte was found one hour after the infection (Figure 7. D). To conclude, the amount of SeV protein increased as the infection progressed and after one hour onwards the proteins were concentrated more in the cells rather than scattered around the cells meaning that the virus had most probably entered the cell by that time.

## 3.5 Viral protein expression levels following SeV infection

Once the virus has managed to enter the host cell, it starts the next step in its life cycle: the replication. The viral protein expression levels after SeV-infection were studied with immunoblotting in order to see if and at what rate the virus is replicating in the cells. The cells were infected with SeV at a MOI of 180 (MOCK cells were uninfected). The cells were lysed, and total proteins were collected at different time points after the infection. Total protein concentration was measured with detergent compatible Bradford assay. For the assay, each standard sample was done with three and unknown protein sample with two replicates and the absorbance of them was measured at 595 nm. Immunoblotting was used to analyze the protein samples. The membrane was stained with polyclonal anti-SeV and a known ladder was used to determine the size of the found protein. The picture of the complete membrane is in attachments (Attachment 5). The anti-GAPDH stain, which serves as a loading control, is from the other membrane that was run at the same time as this anti-SeV experiment. The stained viral proteins of interest on the membrane are seen in the figure 8 and the sizes were compared to a known protein ladder.
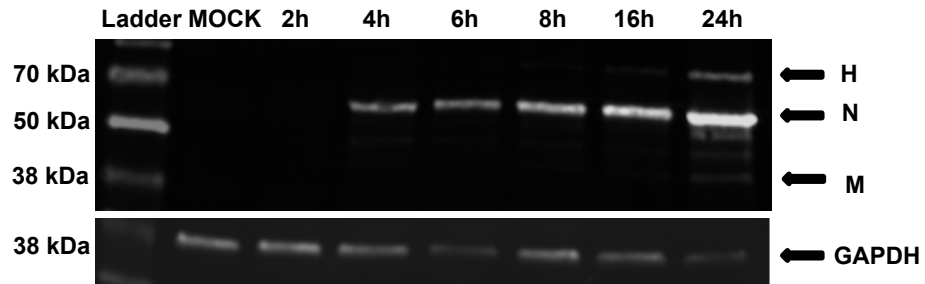
Figure 8. Expression of SeV proteins in infected A549 cells. The cells were infected with a SeV MOI 180 and at different time points (2h, 4h, 6h, 8h, 16h, 24h) they were lysed and total proteins were collected. As a control, uninfected MOCK sample was also collected. Twenty µg of protein per sample were separated on an SDS-PAGE gel and transferred to a nitrocellulose membrane, which was stained with anti-SeV polyclonal antibody. The GAPDH bands are from another membrane (Figure 9), which was run parallel to this membrane and loaded with the same amount of protein. The corresponding proteins are indicated with arrows on the right and the ladder bands of known sizes are presented on the left.

The MOCK sample is clear from any stained proteins, so there was no unspecific staining. A protein approximately 60 kDa in size, which corresponds to SeV N protein, was found from every sample, excluding the MOCK and 2h samples. In addition, a protein approximately 72 kDa in size, which corresponds to the SeV HN protein, was observed 16h (slightly) and 24h after the infection. Additionally, 24h after the infection, there were some smaller and dimmer protein bands to be seen. One of them was about 35 kDa in size, which corresponds to the SeV M protein, and the other one was about 44 kDa in size and unrecognizable and possibly a degeneration product. Conclusively, the amount of SeV proteins increased as the infection progressed. Taken together, since the amount of SeV proteins increased notably as the infection progressed, the virus was able to replicate efficiently in the host cells and this replication was the most efficacious between 16h and 24h after the infection.

## 3.6 Host protein expression levels following SeV infection

Cells express IRF3 constitutively and when it is in an inactive form, it locates in the cytoplasm. The expression levels of IRF3 as well as possible changes in the expression after SeV-infection was studied with immunoblotting in order to characterize more of the effects SeV-infection has to the host cells. The cells were infected with SeV at a MOI of 180 (MOCK cells were uninfected). The cells were lysed, and total proteins were collected at different time points after the infection. Like previously, the total protein concentration was measured with detergent compatible Bradford assay. For this assay, each standard sample was done with three and unknown protein

sample with two replicates and the absorbance of them was measured at 595 nm. The protein samples were analyzed by immunoblotting. The membrane was stained with polyclonal anti-IRF3 antibody and with anti-GAPDH, and a known ladder was used to determine the size of the found protein. The picture of the complete membrane is in attachments (Attachment 6). IRF3 is about 52 kDa in size, which corresponds to the size of a protein found in every sample in the immunoblot (figure 9).
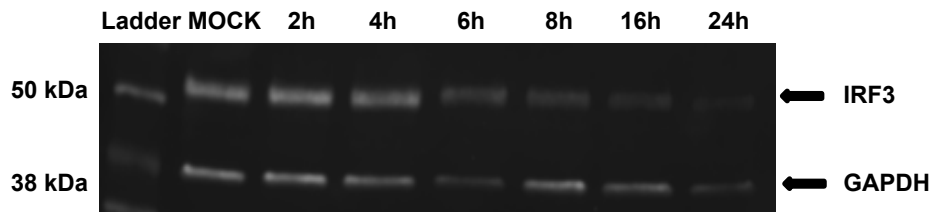


Figure 9. Expression of IRF3 in infected A549 cells. The cells were infected with SeV Cantell strain at a MOI 180 and at different time points (2h, 4h, 6h, 8h, 16h, 24h) cells were lysed and total proteins were collected. As a control, uninfected MOCK sample was also collected. From the samples, containing 20 µg of protein per sample, relative expression levels of IRF3 protein was analyzed by immunoblotting. The membrane was stained with anti-IRF3 monoclonal as well as with GAPDH that functioned as a loading control. The corresponding proteins are indicated with arrows on the right and the ladder bands of known sizes are presented on the left.

GAPDH is about 37 kDa in size, which corresponds to the size of the other protein found in every sample in the immunoblot. Since only those two proteins were observed, there was no unspecific staining. The GAPDH served as a loading control. Based on the GAPDH levels of the samples in the immunoblot, the loading of the samples was even. Since a protein roughly 50 kDa in size was found in every sample in the immunoblot, it indicates that IRF3 was present in every sample. The amount of the 50 kDa protein in the immunoblot were the highest at the early times of the infection (MOCK, 2h, and 4h). Therefore, the protein expression level of IRF3 was the highest at the early times of the infection (MOCK, 2h and 4h). The amount of the 50 kDa protein, i.e. IRF3, decreased as the infection progressed and the decreasing started between four and six hours after the infection. By 24h after the infection, the amount of the 50 kDa protein, i.e. IRF3, had decreased drastically. To conclude, IRF3 started to degrade between four and six hours after the SeV-infection and by 24h after the infection the amount of IRF3 was drastically decreased.

## 3.7 Cytokine and viral mRNA expression in SeV-infected A549 cells

In a virus infection host cell tries to eliminate the virus by producing cytokines that function in eliciting an antiviral state. One group of cytokines is IFNs that

further can be divided into different types. For example, type I IFNs, like IFN$\beta$, are especially important in virus infections. *IFN$\beta$1*, *IFN$\lambda$1* and SeV N protein encoding mRNA expression level changes after SeV-infection were studied with qRT-PCR with specific Taqman™ probes. The cells were first infected with SeV at different MOI values (MOCK cells were uninfected) and lysed, and total RNA was extracted at different time points after the infection. In addition, an experiment where cells were treated with CHX before and during the infection at a MOI of 1 (MOCK cells were uninfected) was done. Exactly like the CHX untreated cells, the CHX treated cells were lysed, and total RNA was extracted at different time points after the infection.

From the RNA samples, cDNAs were made in an RT reaction. The cDNAs were then run in duplicates in qRT-PCR with the specific probes for *IFN$\beta$1*, *IFN$\lambda$1*, and SeV N protein encoding mRNA. Reference gene *GAPDH* (1x mix Hs02758991_g1 GAPDH, Thermo Fisher scientific), and nuclease-free water, and PCR mix controls, i.e. no-template controls, were also included in the run. The used TaqMan™ Gene Expression Assay mixture contains unlabeled sense(s) and antisense (a) primer and a TaqMan probe. The probe has a 6-FAM (emission max 517 nm) dye label and a non-fluorescent quencher molecule on the 5' and 3' ends, respectively. The obtained qRT-PCR results were normalized and calibrated with a $\Delta\Delta C_T$-method, which gives the relative amount of the specific target gene normalized to the reference gene and relative to a calibrator (Livak and Schmittgen 2001). Thus, the results demonstrate a fold change in the gene of interest in relation to the calibrator. In addition of the concentration, the quality (the 260/230 nm and 260/280 nm ratios) of the extracted total RNA was assessed. Despite the fact that some of the samples had small impurities, all the samples were included in the qRT-PCR. The RNA extraction of 16h timepoint sample in SeV infected A549 cells was unsuccessful and due to low RNA gain, comparable qRT-PCR assay was not possible. Similar limitation was experienced with the 24h CHX-treated cells, which was most likely due to the toxicity of CHX as a long-term treatment.

### 3.7.1 SeV N protein encoding mRNA expression after SeV-infection

Once SeV is in the host cell, it seeks to start replication and the production of progeny viruses. The changes in the SeV N protein encoding mRNA expression was studied with qRT-PCR after SeV-infection so that the

possible replication of the virus in the host cells could be assessed. The cells were infected at a MOI of 5 and 50 (MOCK cells were uninfected) and total RNAs were extracted at different time points after the infection. For the RNAs a RT reaction was carried and for the obtained cDNAs a qRT-PCR run performed with a specific primer for the SeV N protein encoding mRNA. For the results, the 30 min SeV N sample was used as a calibrator since it represents the virus that has attached to and moved into the cells early. In both the MOI 5 and MOI 50 SeV-infections, the viral N protein encoding mRNA expression was elevated as the infection progressed (Figure 10).

**Sendai N protein encoding mRNA expression fold changes after SeV MOI 5 and MOI 50 infections in A549 cells**
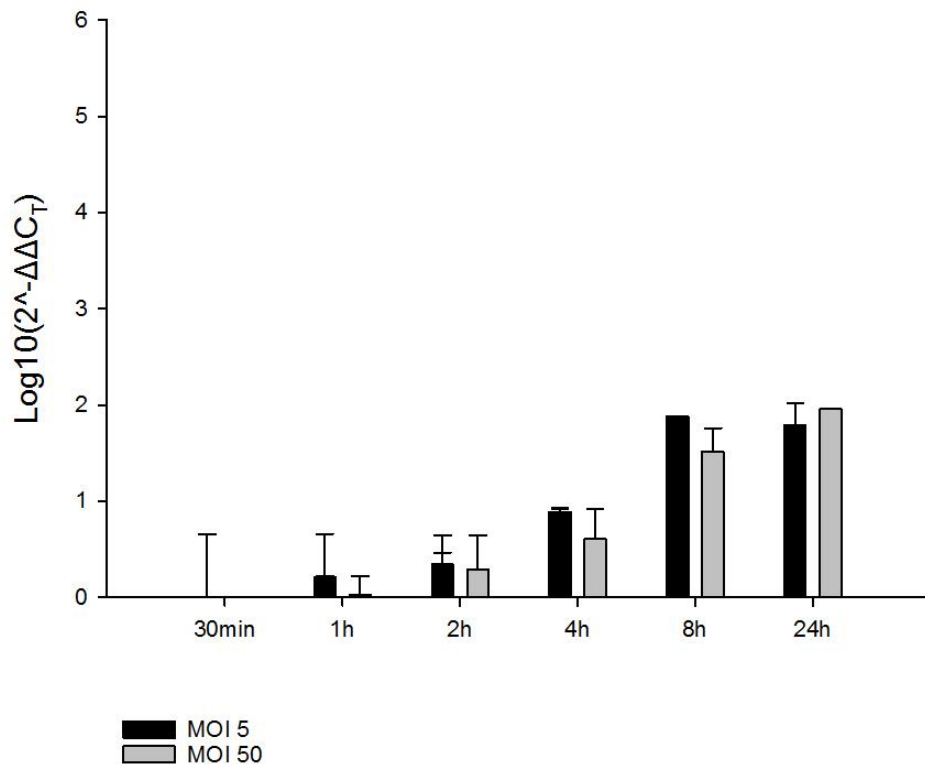


Figure 10. Expression of SeV N protein encoding mRNA in infected A549 cells. Sendai N protein encoding mRNA expression changes, calibrated to the expression of the 30min SeV-infected sample by $\Delta\Delta C_T$-method, from SeV MOI 5 and MOI 50 infected A549 cells obtained by qRT-PCR and run in duplicates. The samples were collected at different time points (30min, 1h, 2h, 4h, 8h and 24h). Q-PCR analyses were performed with specific primers for the gene of interest, SeV *N*, and *GAPDG*. The result of each sample was normalized with *GAPDH* expression. Standard error is shown.

However, there was a minor decreasing in the expression 24h after the MOI 5 SeV-infection when compared to the 8h MOI 5 infection. A slight increase was noticed already one hour after the infection. By four hours after the infection the expression had increased 10-fold. Among the MOI 5 and 50

SeV-infections, the highest expression, was obtained eight hours (about 100-fold increase) and 24h (about 100-fold increase) after the infection, respectively. Importantly, the activation of the SeV N protein encoding mRNA expression followed similar kinetics in both MOI 5 and MOI 50 samples: Increasing of the expression was noticed already after one hour of the infection, and the expression rose steadily. The results demonstrate that the virus was replicating efficiently in the cells since the amount of the viral N protein encoding mRNA increased as the infection progressed, and the increasing started properly between four and eight hours after the infection. In addition, the results show that the MOI had no effect on the replication kinetics nor had it a great effect to the mRNA expression level of the gene at different times in the infection.

### 3.7.2 The *IFN-β1* mRNA expression after SeV-infection

IFNs mediate antiviral effects in viral infections and are important in the clearance of the infective virus. Therefore, in order to characterize more the innate immunity activation after SeV-infection, the *IFN-β1* mRNA expression after SeV-infection was studied with qRT-PCR. More specifically, in order to see if and when a type I IFN is activated after the infection. The cells were infected at a MOI of 5 (MOCK cells were uninfected) and total RNAs were extracted at different time points after the infection. The RNAs were converted into corresponding cDNAs in a RT reaction. The cDNAs were run in qRT-PCR with a specific primer for the *IFN-β1* gene. The results were calibrated to the MOCK values. The *IFN-β1* mRNA expression was increased already 30min after the infection, so the expression started rapidly after the infection and increased steadily (Figure 11).
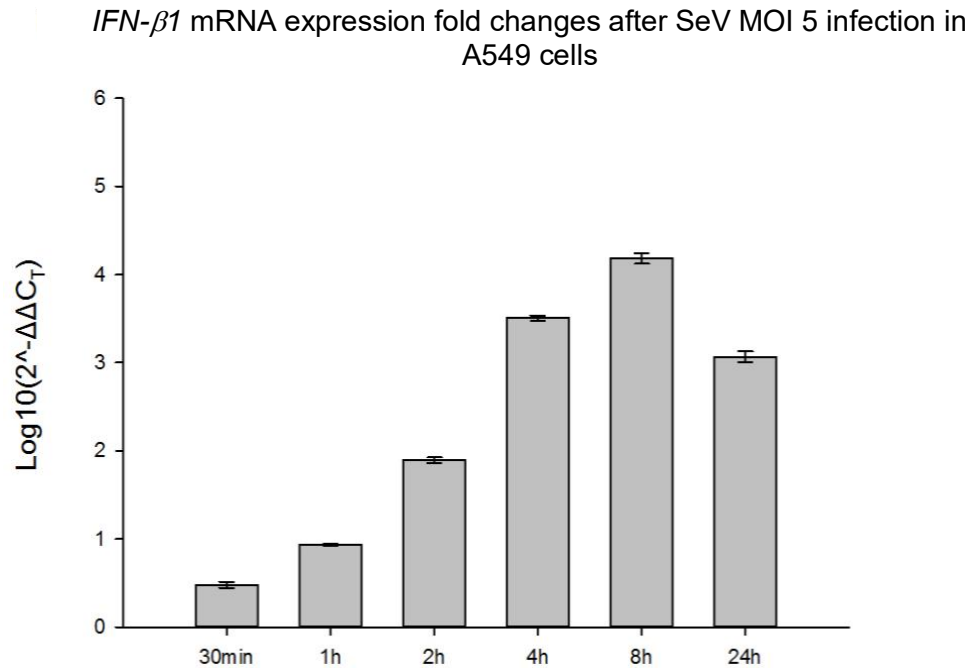
Figure 11. Expression of *IFN-β1* gene in infected A549 cells. *IFN-β1* mRNA expression changes, calibrated to the expression of the MOCK sample by ΔΔC_T-method, from SeV MOI 5 infected A549 cells obtained by qRT-PCR and run in duplicates. The samples were collected at different time points (30min, 1h, 2h, 4h, 8h and 24h). Q-PCR analyses were performed with specific primers for the gene of interest, *IFN-β1*, and *GAPDG*. The result of each sample was normalized with *GAPDH* expression. Standard error is shown.

It peaked at eight hours after the infection and started to decline between eight and 24h after the infection. To conclude, the *IFN-β1* mRNA expression was upregulated throughout the infection, and the upregulation occurred rapidly and rose quickly from 100-fold two hours after the infection to 100000-fold eight hours after the infection. The results state that the possible antiviral effect, the expression of *IFN-β1* gene, started properly between one and four hours after infecting the cells with SeV and the expression was efficient and rose up to 100000-fold.

3.7.3 The *IFN-ƛ1* mRNA expression after SeV-infection

Further, the antiviral effects mediated by IFNs are important in the clearance of the virus and in the recovery of the host. Therefore, a type III IFN, *IFN-ƛ1*, mRNA expression levels after SeV-infection were studied with qRT-PCR in order to study if and when this expression starts after SeV-infection. The cells were infected at a MOI of 5 (MOCK cells were uninfected) and total RNAs were extracted from the cells and reverse transcribed into cDNAs. The cDNAs were run in qRT-PCR with a specific primer for the *IFN-ƛ1* gene. The expression of *IFN-ƛ1* in MOCK cells was minor and therefore undetected.

Hence, the results were calibrated to the 30 min IFN-λ1 ones rather than to the MOCK values. The *IFN-λ1* mRNA expression was increasing as the infection progressed (figure 12).
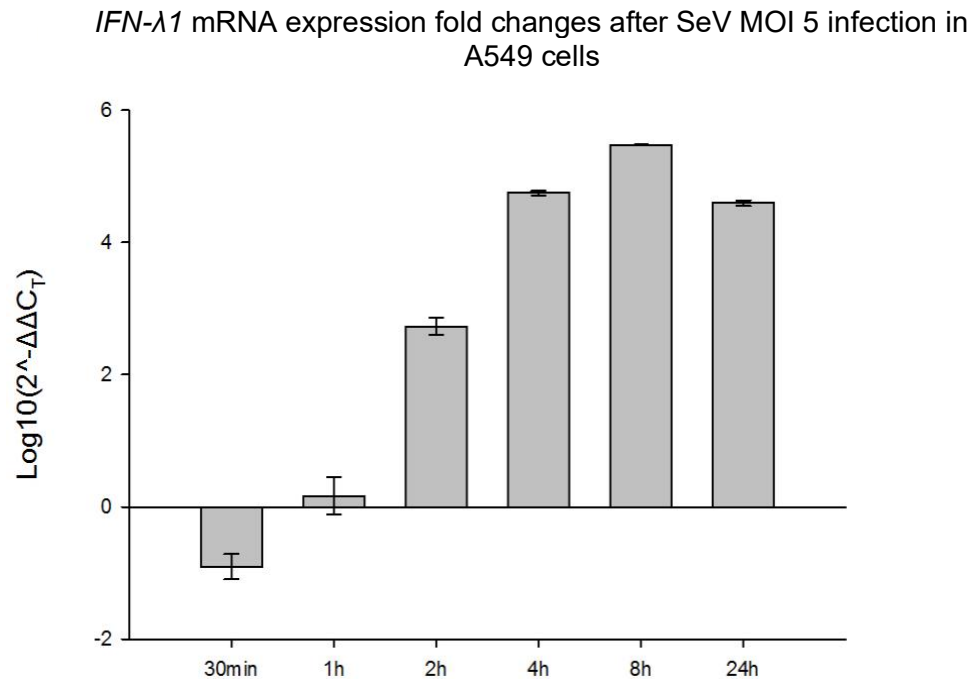
**IFN-λ1 mRNA expression fold changes after SeV MOI 5 infection in A549 cells**



Figure 12. Expression of *IFN-λ1* gene in infected A549 cells. *IFN-λ1* mRNA expression changes, calibrated to the expression of the 30min sample by ΔΔCT-method, from SeV MOI 5 infected A549 cells obtained by qRT-PCR and run in duplicates. The samples were collected at different time points (30min, 1h, 2h, 4h, 8h and 24h). Q-PCR analyses were performed with specific primers for the gene of interest, *IFN-λ1*, and *GAPDG*, which was the reference gene. The result of each sample was normalized with *GAPDH* expression. Standard error is shown.

The expression jumped significantly within one to two hours after the infection: from about 10-fold to almost 1000-fold. The expression peaked eight hours after the infection (over 1000000-fold) and started to decline between eight hours to 24h after the infection. To conclude, excluding 30 min after the infection, the *IFN-λ1* mRNA expression was upregulated quickly and efficiently as the infection progressed. Therefore, the possible antiviral effect, the expression of the *IFN-λ1* gene after SeV-infection started properly between two to four hours after the infection.

3.7.4 SeV N protein encoding mRNA expression after SeV-infection when protein synthesis is blocked

The invaded virus uses the host's replication machinery to replicate itself. The expression changes of viral N protein encoding mRNA after SeV-infection were studied with qRT-PCR with CHX+ cells in order to demonstrate if the possible virus replication is efficiently blocked with CHX. The cells were

treated with CHX before and during the infection at a MOI of 1 (MOCK cells were uninfected). The total RNAs were extracted at different time points after the infection. The RT reaction for the RNAs was done. The obtained cDNAs were run in qRT-PCR with a specific primer for the SeV N protein encoding sequence. The results were calibrated to the 30 min SeV N sample values, since it represents the virus that has attached to and moved into the cells early. The SeV N protein encoding mRNA expression nearly peaked between two and four hours after the infection (figure 13).

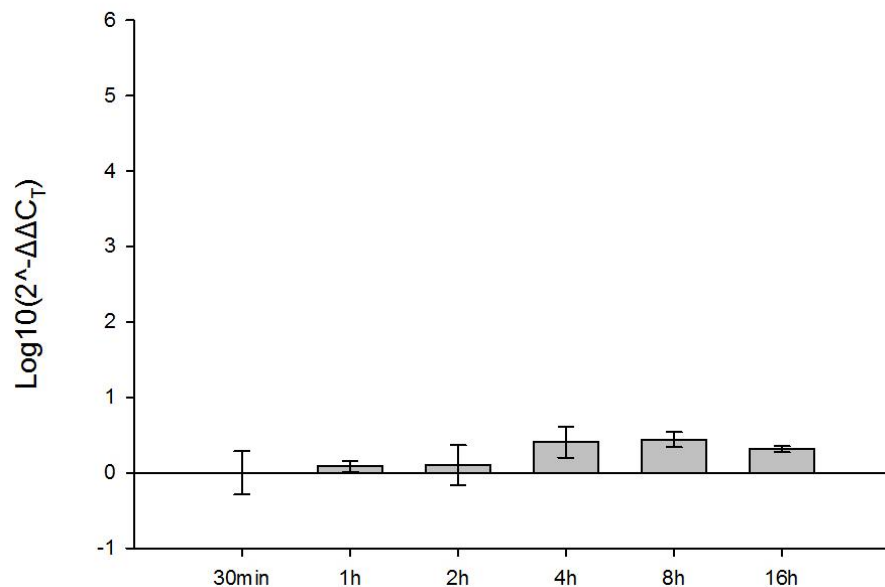Sendai N protein encoding mRNA expression fold changes after SeV MOI 1 infection in A549 CHX+ cells



Figure 13. Expression of SeV N protein encoding mRNA in infected A549 cells treated with CHX. Sendai N protein encoding mRNA expression changes, calibrated to the expression of the 30min SeV-infected sample by $\Delta\Delta C_T$-method, from SeV MOI 1 infected A549 cells that were treated with CHX, obtained by qRT-PCR and run in duplicates. The samples were collected at different time points (30min, 1h, 2h, 4h, 8h and 16h). Q-PCR analyses were performed with specific primers for the gene of interest, SeV *N*, and *GAPDG*, which was the reference gene. The result of each sample was normalized with *GAPDH* expression. Standard error is shown.

Nonetheless, about five-fold increase, so the highest viral N protein encoding mRNA expression, was eight hours after the infection. Then again, at 16h after the infection, the expression was lower compared to after eight hours. Importantly, when these results are compared to the CHX- ones, the peak expressions had 1,5 times difference between CHX- and CHX+ cells (figure 10 and 13). Therefore, it is clear that the viral N protein encoding mRNA expression was greatly repressed in the CHX+ cells. To conclude, the viral N protein encoding mRNA expression was only somewhat upregulated as the infection progressed and started to decline between eight and 16h after the

infection (figure 13). The results demonstrate that when cells were treated with CHX, the virus replication was efficiently compromised.

3.7.5 The *IFN-β1* mRNA expression after SeV-infection when protein synthesis is blocked

Further, in a virus infection, the efficient activation of IFN production is crucial in the clearance of the virus. Therefore, the *IFN-β1* mRNA expression levels after SeV-infection were studied with qRT-PCR to see if and when the *IFN-β1* mRNA expression starts after SeV-infection when the protein synthesis is blocked with CHX. The cells were treated with CHX before and during the infection at a MOI of 1 (MOCK cells were uninfected). The total RNAs were extracted at different time points after the infection and reverse transcribed into cDNAs. The cDNAs were run in qRT-PCR with a specific primer for *IFN-β1* gene. The results were calibrated to the MOCK values. The *IFN-β1* mRNA expression was a bit miscellaneous: First it was increasing (1h) followed with a slight decrease (2h) compared to the expression at one hour, and then again increasing (4h and 8h) and finally decreasing (16h) when compared to eight hours (figure 14).

*IFN-β1* mRNA expression fold changes after SeV MOI 1 infection in A549 CHX+ cells



Figure 14. Expression of *IFN-β1* gene in infected A549 cells treated with CHX. *IFN-β1* mRNA expression changes, calibrated to the expression of the MOCK sample by $\Delta\Delta C_T$-method, from SeV MOI 1 infected A549 cells that were treated with CHX, obtained by qRT-PCR and run in duplicates. The samples were collected at different time points (1h, 2h, 4h, 8h and 16h). Q-PCR analyses were performed with specific primers for the gene of interest, *IFN-β1*, and *GAPDG*, which was the reference gene. The result of each sample was normalized with *GAPDH* expression. Standard error is shown.

The expression increased about 50-fold eight hours after the infection, and that was the peak of the expression. On the other hand, the *IFN-β1* mRNA expression was upregulated in every sample after the infection, and the expression started quickly and rose as the infection progressed. To conclude, even when protein synthesis was blocked the possible antiviral effect of the expression of the *IFN-β1* gene after SeV-infection started early in the infection, properly between two to four hours after the infection.

3.7.6 The *IFN-ƛ1* mRNA expression levels after *SeV*-infection when protein synthesis is blocked

The importance of the production of IFNs in response to a virus infection and in the elimination of the virus is well known. Therefore, to study if and when a type III IFN, IFN-ƛ1, expression starts after SeV-infection when protein synthesis is blocked, *IFN-ƛ1* mRNA expression levels of SeV-infected CHX+ cells were analyzed by qRT-PCR. The cells were treated with CHX before and during the infection at a MOI of 1 (MOCK cells were uninfected). Like previously, the total RNAs were extracted at different time points after the infection, and they were reverse transcribed into cDNAs. The cDNAs were run in a qRT-PCR with a specific primer for *IFN-ƛ1* gene. The results were calibrated to the 30 min IFN-λ1 sample values, since MOCK level *IFN-ƛ1* expression was unobtained. As seen from the figure 15, the *IFN-ƛ1* mRNA expression was increasing as the infection progressed, excluding the result after one hour, until it started to decline 16h after the infection when compared to the expression eight hours after the infection.

IFN-λ1 mRNA expression fold changes after SeV MOI 1 infection in A549 CHX+ cells
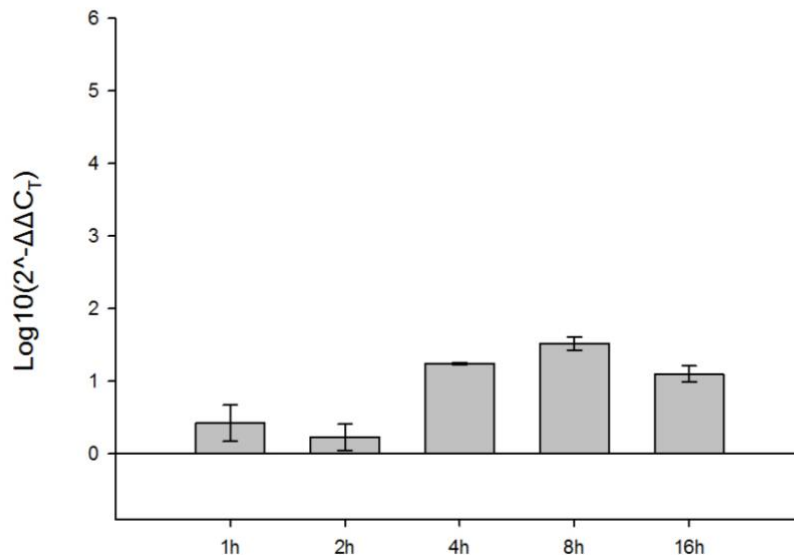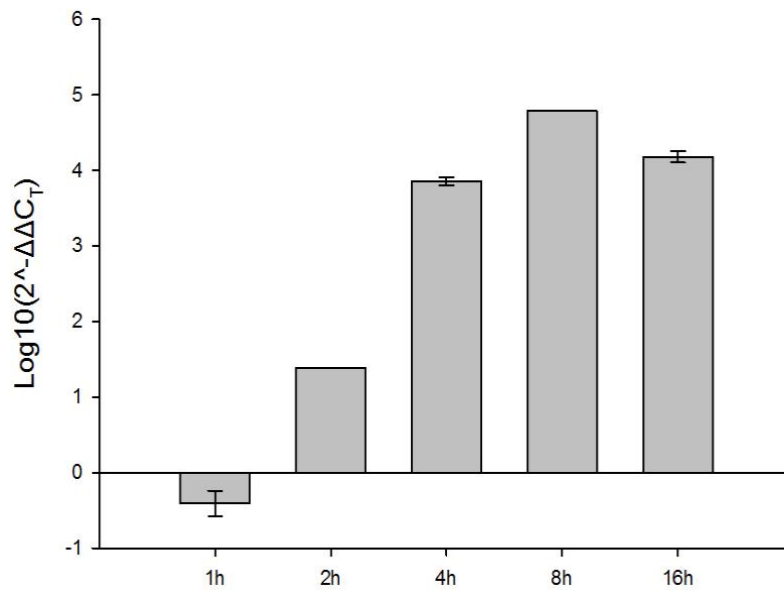
Figure 15. Expression of *IFN-λ1* gene in infected A549 cells treated with CHX. *IFN-λ1* mRNA expression changes, calibrated to the expression of the 30min sample by ΔΔCT-method, from SeV MOI 1 infected A549 cells that were treated with CHX, obtained by qRT-PCR and run in duplicates. The samples were collected at different time points (1h, 2h, 4h, 8h and 16h). Q-PCR analyses were performed with specific primers for the gene of interest, *IFN-λ1*, and *GAPDG*, which was the reference gene. The result of each sample was normalized with *GAPDH* expression. Standard error is shown.

The peak expression obtained was at eight hours after the infection. In conclusion, the *IFN-λ1* mRNA expression was upregulated fast and greatly (about 100000-fold) as the infection progressed and the expression started to decline between eight and 16h after the infection. Hence, the possible antiviral effect of the expression of the *IFN-λ1* gene after SeV-infection started even when protein synthesis was blocked, and the effect occurred between two to four hours after the infection.

## 4. Discussion

The goal of this study was to examine the activation kinetics of the Rig-I pathway after sendai virus infection in human adenocarcinomic lung epithelial A549 cells. Additionally, the central aim was to study if the entry of the virus into the cell would be sufficient to activate the Rig-I pathway or whether the virus needs to replicate first before it can elicit the activation. This study showed that IRF3 was translocating from cytoplasm into the nucleus and thus activated quickly after SeV-infection. This activation of

IRF3 was followed by efficacious induction of *IFN-β1* and *IFN-λ1* mRNA expressions. Furthermore, IRF3 was degraded as the SeV-infection progressed. In addition, CHX blocked SeV replication efficiently. Nevertheless, in the CHX treated cells the *IFN-β1* and *IFN-λ1* mRNAs were expressed efficiently and IRF3 translocated into the nucleus. Therefore, the activation of these innate immunity responses after SeV-infection were independent of the virus replication.

This study is addressing the requirements of activation of specific innate immunity responses, the translocation of IRF3 and IFN mRNA expressions, after SeV-infection with whole virus *in vitro* infection experiments. The cells were infected with SeV Cantell strain at certain MOI values and samples (whole cells, total RNA, total protein) were collected at different time points after the infection and analyzed. The tools to study the research questions were to focus in the expression and localization of IRF3, which is a transcription factor at the bottom of the Rig-I signaling pathway cascade (Peters et al. 2008; Hare and Mossman 2013), as well as in the expression of IFN and viral mRNAs and proteins after SeV-infection.

There are many references that in nonimmune cells, like A549 cells, Rig-I is the fundamental PRR in SeV-infection (Kato et al. 2005; Melchjorsen et al. 2005; Loo et al. 2008). In addition, it has been shown that in SeV-infection, the Rig-I is essential for type I and III IFN (IFN-β and IFN-λ1) activation and regulation (Kato et al. 2006; Österlund et al. 2007). However, PRRs are known to function cell-type specifically and cooperatively (Melchjorsen et al. 2005; Medzhitov 2007). Importantly, MDA5, but not Rig-I, is known to be inhibited by SeV V protein (Childs et al. 2007), which is a factor supporting the fact that the activation of IRF3 after SeV-infection is indeed mainly upstream of Rig-I rather than MDA5. Since TLRs mainly recognize nucleic acids in extracellular space or in endosomes (Mogensen and Paludan 2005), it is also from this point of view most likely Rig-I that is sensing SeV residing in the cytosol. Consequently, it was presumed in this study that Rig-I is activated after SeV-infection, even though this study lacks Rig-I knockout cell line experiments to prove it definitely.

The virus stock that was used in the experiments was effective to activate antiviral effects in the cells as the FFU / ml value was as high as $6 \times 10^9$. The result is really high (Veckman et al. 2006), which may indicate that the SeV

stock titer estimation protocol had some imprecisions. Behind this is probably the way the virus dilutions were prepared in the SeV stock titer experiment: the pipette tips were not changed in between the serial dilution preparation, which may have increased the number of virus in the higher dilution aliquots.

In our experience the A549 cells were not compatible for the PFU assay with AVICEL. Reasons for this are unclear and unexpected. All cells were detached in the PFU assay, both MOCK and the infected cells. AVICEL in general is an overlay solution that prevents the virus from spreading in the cell culture and thus facilitates the determination of the virus titer by counting the formed holes, which are a result of cell death, in the cell layer. Overall, more optimization is needed regarding the PFU assay. The benefits of FFU assay when compared to PFU assay are that it is more sensitive and not as time consuming (Baer and Kehn-Hall 2014), which therefore address its suitability in evaluating the MOI values in the infection experiments.

The results from the infection experiments showed that the Rig-I pathway was activated rapidly, already an hour after the SeV-infection, which was confirmed with the immunofluorescence visualization of translocation of IRF3 into the nucleus after the infection. The translocation of IRF3 into nucleus occurred very rapidly when compared to that for example after Newcastle disease virus (NDV), another paramyxovirus, which occurs 12h after the infection (Sato et al. 1998). In addition, Sato et al. (1998) found that the virus (NDV) needs to replicate to be recognized by the Rig-I and MDA5, which probably is the reason for slower IRF3 translocation kinetics. In my experiment, the used MOI was really high (3700), which means that there were plenty of viruses in the cells. This may have resulted in faster activation of the Rig-I pathway.

Possible translocation of IRF3 into nucleus after SeV-infection was studied also with cells treated with CHX by immunocytochemical staining. CHX inhibits *de novo* protein synthesis (Wettstein et al. 1964; Schneider-Poetsch et al. 2010). Since SeV carries an *RNA-dependent RNA polymerase* gene in its genome, it can synthetize some primary transcription products even in the presence of CHX, which inhibits host cell protein synthesis (Robinson 1971; Kolakofsky et al. 2004; Schneider-Poetsch et al. 2010). However, complete and large-scale replication of viruses is still inhibited with CHX (Robinson 1971; Murphy and Lazzarini 1974; Weber et al. 2013). The

immunocytochemical staining experiments with CHX treated cells showed that IRF3 translocated into nucleus and that this localization shift happened already one hour after the infection. Thus, these results from CHX+ and CHX- cells are alike. This supports the hypothesis that SeV does not have to replicate before the recognition by the Rig-I. Likewise, Collins et al. (2004) showed that cells treated with CHX had raised levels of activated IRF3 after SeV-infection. Interestingly, opposite results have also been obtained. When Melchjorsen et al. (2005) infected cells with UV-inactivated SeV (Cantell strain, MOI 1), which lacked the ability to replicate, the activation of IRF3 was completely abolished. On the other hand, there is a difference between inactivation of the virus by UV light or inhibiting the replication of the virus by CHX. UV treatment may damage the overall structure of the virus particle (Miller and Plagemann 1973; Lovinger et al. 1975) whereas CHX only inhibits the virus replication indirectly by disabling the protein synthesis machinery of the host (Wettstein et al. 1964; Schneider-Poetsch et al. 2010). However, the results are opposing and further investigation on the matter should be executed.

The results from the immunoblot assay showed that IRF3 began to degrade between four and six hours after the SeV-infection and from there on, this degradation continued throughout the followed time course of the infection. The amount of IRF3 was nearly diminished by 24h after the infection. Therefore, SeV-infection induced the degradation of IRF3. Similar kind of result were obtained in a study made by Lin et al. (1998) where SeV-infection was shown to lead to degradation of IRF3 16h after the infection. In an experiment made by Collins et al. (2004) IRF3 degradation in SeV-infected A549 cells occurred even earlier, by 12h post infection. However, in my results, the degradation occurred even earlier. This could mean that the infection in my experiment was more efficient than in the Lin et al. (1998) and in Collins et al. (2004) experiments where used MOI was significantly lower or simply due to the lack of earlier time points in those two other experiments. From mutation experiments, it is concluded that the phosphorylation of IRF3, i.e. its activation, would be the activator signal for its degradation (Lin et al. 1998). This is so, because phosphorylation is a signal for ubiquitin-dependent proteasome degradation (Bibeau-Poirier et al. 2006). Consequently, the rapid degradation of IRF3 in my results indicates that the activation of innate immunity response by SeV-infection was efficient.

In the immunoblot experiment, polyclonal antibody against IRF3 was used. The size of phosphorylated IRF3 should be dissimilar to the constitutively expressed IRF3 (Servant et al. 2001). However, in my experiments no change in size of the found IRF3 was observed when MOCK and SeV-infected cells were compared. Therefore, for better accuracy, an antibody against the phosphorylated form of IRF3 would be needed. Importantly, in the immunoblot assay the used MOI was 180, which is only a fraction of the one in the immunocytochemical staining experiments. Therefore, the finding made from the immunocytochemical staining experiment about the rapid activation of the Rig-I seems to be valid regardless of the very high MOI used in that experiment.

In the other immunoblot assay stained with polyclonal anti-SeV, SeV proteins were starting to increase between six and eight hours after the infection and peaked within 24h after the infection. In addition, the first sign of SeV proteins was detected only four hours after the infection while MOCK and the sample collected two hours after the infection lacked detectable SeV protein bands. It is peculiar that two hours after the infection SeV proteins were undetectable, since the data from the immunocytochemical staining experiments of CHX- cells against polyclonal anti-SeV showed that SeV proteins started to properly accumulate in the cells after one hour of the infection, which indicates that SeV moved into the cells already within one hour after the infection. Moreover, from the experiments, possible polycaryocyte and rounding of cells were also seen one hour after the infection. These morphological changes are signs of cytotoxic effects of SeV infection. This indicates that the cells were indeed infected by that time. Unfortunately, double staining experiment against both IRF3 and SeV proteins could not be performed since both antibodies in use were raised in rabbits. Moreover, in the immunoblot assay, the amount of SeV proteins between four and six hours remained unchanged. This strongly suggests that between four and six hours after the infection, only the incoming virus was detected, and the virus was not yet replicating. These notions further substantiate the conclusion made from the anti-IRF3 immunocytochemical staining experiments that the Rig-I pathway was activated independent of SeV replication.

The expression of SeV N protein encoding mRNA, which precedes the replication, in CHX- cells started properly between two to four hours after the

infection, based on the qRT-PCR results. This is in line with the other results, since protein expression takes longer than mRNA expression, and the protein expression levels of SeV were properly accumulating in the immunoblot assay between 16h and 24h after the infection. Like noted regarding the anti-SeV immunoblot results, the slight increased signal at 30min to two hours was likely from the incoming virus. In MOI 5 and MOI 50 CHX- cells, the expression reached 100-fold increase between four and eight hours and eight and 24 hours, respectively. Thus, the higher MOI value seemed to be slowing the induction of the virus N protein encoding mRNA expression a bit in this experiment. This is supporting the point made regarding the earlier activation of the Rig-I because of high MOI (3700) in the immunological staining experiments: perhaps the virus was not replicating as quickly in higher MOI values because it was recognized earlier due to greater accumulation of virus particles in the host cell at the beginning of the infection. On the other hand, this difference in induction of the viral N protein encoding mRNA expression between MOI 5 and MOI 50 CHX- cells was fairly minimal. The SeV *N* gene results from CHX+ cells were the opposite showing only slight expressional increase when compared to the CHX- result. This proves that CHX blocked the virus replication efficiently.

IFN production is of great importance in the innate immune system as well as in the activation and modulation of adaptive immunity and ultimately in the clearance of the virus (Medzhitov 2007). It is known that the active transcription factor complex of IRF3 and CBP/p300 can induce IFN gene expression and that this primary expression happens early in the infection (Sato et al. 1998; Yoneyama et al. 1998; Sato et al. 2000; Österlund et al. 2007). Interestingly, in my qRT-PCR results of CHX+ (10 μg / ml) cells, *IFN-β1* and *IFN-λ1* mRNA expressions were increasing as the SeV-infection progresses. Therefore, the innate immunity and antiviral state was activated once SeV was in the host cell and independently of the virus replication. Interestingly, the expression levels of *IFN-β1* CHX- and *IFN-λ1* mRNAs of CHX+ and CHX- cells were similar, while the *IFN-β1* mRNA expression of CHX+ cells differed significantly from all the formerly mentioned ones: the *IFN-β1* mRNA expression of CHX+ cells was significantly lower than the *IFN-β1* CHX- and both the *IFN-λ1* CHX+ and CHX- qRT-PCR results. It remains unclear why in CHX+ cells the *IFN-β1* mRNA expression was significantly lower than the *IFN-λ1* mRNA expression. IFN-β and IFN-λ are activated via different receptors and partially different routes (Abramovich et al. 1994;

Novick et al. 1994; Kotenko et al. 2003; Prokunina-Olsson et al. 2013), which may explain the difference. Maybe CHX can somehow affect only the receptor or route regulating IFN-β, and this aspect requires more research. In the experiment the MOI was really low (MOI 1) and yet effective to activate innate immunity responses when the virus replication was blocked.

On the contrary, in a study by Melchjorsen et al. (2005), the IFN-α and IFN-β production were abolished when cells were infected at a MOI of 1 with UV-inactivated SeV. Additionally, in a study made with another paramyxovirus, RSV, IFN-α production was compromised when cells were infected with inactivated RSV (Hornung et al. 2004). Then again, Weber et al. (2013) got results similar to mine in their experiments that were done with CHX+ (50 µg / ml) A549 cells that were infected with VSV and IAV virus genomes (containing nucleocapsids). In that experiment, the expression level of *IFN-β* in CHX+ cells 24h after the infection was only slightly affected when compared to CHX- ones. They concluded that viral nucleocapsid with 5' triphosphate dsRNA panhandle structure act as the ligand for Rig-I (Weber et al. 2013). The different conclusions from the introduced studies and my study may relate to use of different viruses in the experiments.

It is known that activated IRF3, once it has bind to its co-activators, can bind to ISREs (Au et al. 1995). In a study by Österlund et al. (2007) the binding of phosphorylated IRF3 in an ISRE element occurred two hours after the SeV-infection in moDCs. Therefore, in moDCs the transcription factor function of IRF3 seems to be activated only two hours after the infection. My results showed that the *IFN-β1* and *IFN-λ1* mRNA expressions were starting to properly increase between two to four hours (except the *IFN-β1* expression of CHX- cells that was increasing properly already one hour after the infection). This is supporting the finding about the kinetics of phosphorylated IRF3 binding in ISRE that Österlund et al. (2007) made. In my results, the increase that was observed earlier than two hours after the infection was minor. Since it is known that cytokines are expressed at low levels even without an infection (Tovey et al. 1987), the signal from the early hours might be due to this constitutive low-level expression of IFNs.

The peak of *IFN-β* and *IFN-λ1* in this study was between six and eight hours after the infection. At the peak of the expression, the expression fold increase of both IFNs in CHX- and CHX+ cells were over 100000. This indicates that

SeV was able to induce IFN expression very efficiently, which is shown also by previous studies (Cantell et al. 1981; Cantell and Hirvonen 1981). The corresponding peak of the same IFNs in the Österlund et al. (2007) study occurred somewhat earlier, six hours after the SeV-infection. Since in my study qRT-PCR results of six hours' time points were lacking, the IFN peaks could be the same as in the Österlund et al. (2007) study. The MOI values of my CHX- and CHX+ results and results from Österlund et al. (2007) study are the same or almost the same, so the earlier activation of IFNs in the Österlund et al. (2007) study is explained by some other reason.

It is known that SeV V protein can inhibit IFN-$\beta$ production (Poole et al. 2002; Andrejeva et al. 2004; Komatsu et al. 2004). In addition, in experiments using mutated and wt SeV conducted by Strähle et al. (2003), IFN-$\beta$ production after SeV (wt) infection is shown to be relatively weak (Strähle et al. 2003). The data I got from qPCR analysis is for some part in line with this finding, since *IFN-$\beta$1* expression was lower than *IFN-$\lambda$1* expression. Likewise, in the study by Österlund et al. (2007) *IFN-$\lambda$* expression was shown to be greater than *IFN-$\beta$* expression after MOI 5 SeV Cantell infection. Furthermore, also in the study by Jiang et al. (2011), the mRNA expression of *IFN-$\beta$* was lower than the expression of *IFN-$\lambda$1* mRNA.

If SeV, a ss(-)RNA virus, elicited Rig-I activation even without replication, the ligand for Rig-I most likely is the incoming virus nucleocapsid or the revealed genome. Oh et al. (2016) have proposed that the first transcript product, *le* polypeptide, of NDV, also a negative-sense non-segmented RNA virus, could act as an agonist for Rig-I. However, the activating effect of that might be so delicate that the result is insignificant and interferon production remain low (Oh et al. 2016). This kind of conclusion can be drawn from the results seen in my experiments: *IFN-$\beta$1*, *IFN-$\lambda$1*, and SeV N protein encoding mRNA expressions remained quite low in the early face of the infection (between 30min and one hour) and peaked at eight hours after the infection, while IRF3 was in the nucleus already after one hour. So, the Rig-I pathway was activated rapidly and before proper replication of the virus, therefore, leaning towards argument that the possible Rig-I agonist could be the *le* polypeptide. However, more detailed research is needed in order to draw proper conclusion of the natural ligand of the Rig-I receptor after SeV-infection, since NDV and SeV are however different viruses.

The reason for varying results to some other studies may be related to many variables, for example to the virus stock, cell culture conditions, used antibodies or other reagents. In the qRT-PCR experiment, a baseline for *IFN-λ1* mRNA expression, the MOCK cell IFN-λ1 mRNA expression, was unobtained. Therefore, the *IFN-β1* and *IFN-λ1* qRT-PCR results were calibrated differently. Hence, the accuracy of the comparison of the *IFN-β1* and *IFN-λ1* mRNA expression results after the infection is somewhat impaired.

To conclude, the results of my study showed that SeV activated antiviral state (type I and III IFN mRNA expression), which was likely mediated by activation of IRF3 by the Rig-I. This activation occurred effectively within one hour after the infection, and even if the virus replication was blocked. The rapidly occurring degradation of IRF3 induced by SeV-infection indicates that the activation of innate immunity responses were effective and widespread. Hence, low levels of IRF3 in the nucleus early after the SeV-infection was enough to activate efficient antiviral responses in the host cell.

Since SeV shares similar functioning mechanisms with other paramyxoviruses that cause diseases in humans such as human parainfluenza virus type I (hPIV-1) (Gorman et al. 1990; Lyn et al. 1991; Slobod et al. 2004), the data acquired in this study could be beneficial also in understanding functioning mechanisms of other paramyxoviruses. Like with SeV, for hPIV-1 there are currently no vaccines available, so the research is valuable. Sendai virus's capacity in gene therapy has been studied extensively and it is a prominent candidate in many therapy forms (Yonemitsu et al. 2000; Jin et al. 2003; Nakanishi and Otsu 2012, Matveeva et al. 2015; Park et al. 2016). Information on SeV infection mechanism is valuable also on that aspect. Importance for research on interactions between and mechanisms of innate immunity and virus infection are underlined in the present time where the new coronavirus pandemic is causing huge costs on the world's economy as well as panic, and most importantly, human suffering including mortality (European Centre for Disease Prevention and Control, ECDC; Finnish Government; Finnish Institute for Health and Welfare, THL; World Health Organization, WHO). Moreover, infectious diseases are one of the leading causes of deaths in the world (Global Health Observatory, GHO), so studying the mechanisms behind immunity and virus infections are of great importance. To conclude,

this study is important in understanding the early interaction of the host and the virus and therefore beneficial for, for example, endeavors to create effective new antiviral therapies.

# 5. Acknowledgements

# 6. References

BIBLIOGRAPHY

Abramovich C, Shulman LM, Ratovitski E, Harroch S, Tovey M, Eid P, Revel M (1994) Differential tyrosine phosphorylation of the IFNAR chain of the type I interferon receptor and of an associated surface protein in response to IFN-alpha and IFN-beta. *Embo J.* 13: 5871-5877.

Afonso CL, Amarasinghe GK, Banyai K, Bao Y, Basler CF, Bavari S, Bejerman N, Blasdell KR, Briand FX, Briese T, Bukreyev A, Calisher CH, Chandran K, Chéng J, Clawson AN, Collins PL, Dietzgen RG, Dolnik O, Domier LL, Dürrwald R, Dye JM, Easton AJ, Ebihara H, Farkas SL, Freitas-Astúa J, Formenty P, Fouchier RAM, Fù Y, Ghedin E, Goodin MM, Hewson R, Horie M, Hyndman TH, Jiāng D, Kitajima EW, Kobinger GP, Kondo H, Kurath G, Lamb RA, Lenardon S, Leroy EM, Li CX, Lin XD, Liú L, Longdon B, Marton S, Maisner A, Mühlberger E, Netesov SV, Nowotny N, Patterson JL, Payne SL, Paweska JT, Randall RE, Rima BK, Rota P, Rubbenstroth D, Schwemmle M, Shi M, Smither SJ, Stenglein MD, Stone DM, Takada A, Terregino C, Tesh RB, Tian JH, Tomonaga K, Tordo N, Towner JS, Vasilakis N, Verbeek M, Volchkov VE, Wahl-Jensen V, Walsh JA, Walker PJ, Wang D, Wang LF, Wetzel T, Whitfield AE, Xiè JT, Yuen KY, Zhang YZ, Kuhn JH (2016) Taxonomy of the order Mononegavirales: update 2016. *Arch. Virol.* 161: 2351-2360.

Agol VI (1974) Towards the system of viruses. *BioSystems* 6: 113-132.

Akira S, Uematsu S, Takeuchi O (2006) Pathogen recognition and innate immunity. *Cell* 124: 783-801.

Andrejeva J, Childs KS, Young DF, Carlos TS, Stock N, Goodbourn S, Randall RE (2004) The V proteins of paramyxoviruses bind the IFN-inducible RNA helicase, mda-5, and inhibit its activation of the IFN-beta promoter. *Proc. Natl. Acad. Sci. U. S. A.* 101: 17264-17269.

Au WC, Moore PA, Lowther W, Juang YT, Pitha PM (1995) Identification of a member of the interferon regulatory factor family that binds to the interferon-stimulated response element and activates expression of interferon-induced genes. *Proc. Natl. Acad. Sci. U. S. A.* 92: 11657-11661.

Baer A, Kehn-Hall K (2014) Viral concentration determination through plaque assays: using traditional and novel overlay systems. *J. Vis. Exp.* 93.

Baltimore D (1971) Expression of animal virus genomes. *Bacteriol. Rev.* 35: 235-241.

Baum A, Sachidanandam R, Garcia-Sastre A (2010) Preference of RIG-I for short viral RNA molecules in infected cells revealed by next-generation sequencing. *Proc. Natl. Acad. Sci. U. S. A.* 107: 16303-16308.

Beachboard DC, Horner SM (2016) Innate immune evasion strategies of DNA and RNA viruses. *Curr. Opin. Microbiol.* 32: 113-119.

Bibeau-Poirier A, Gravel SP, Clement JF, Rolland S, Rodier G, Coulombe P, Hiscott J, Grandvaux N, Meloche S, Servant MJ (2006) Involvement of the IkappaB kinase (IKK)-related kinases tank-binding kinase 1/IKKi and cullin-based ubiquitin ligases in IFN regulatory factor-3 degradation. *J. Immunol.* 177: 5059-5067.

Bitzer M, Lauer U, Baumann C, Spiegel M, Gregor M, Neubert WJ (1997) Sendai virus efficiently infects cells via the asialoglycoprotein receptor and requires the presence of cleaved F0 precursor proteins for this alternative route of cell entry. *J. Virol.* 71: 5481-5486.

Bousse T, Takimoto T, Gorman WL, Takahashi T, Portner A (1994) Regions on the hemagglutinin-neuraminidase proteins of human parainfluenza virus type-1 and Sendai virus important for membrane fusion. *Virology* 204: 506-514.

Brownell J, Bruckner J, Wagoner J, Thomas E, Loo YM, Gale M,Jr, Liang TJ, Polyak SJ (2014) Direct, interferon-independent activation of the CXCL10 promoter by NF-kappaB and interferon regulatory factor 3 during hepatitis C virus infection. *J. Virol.* 88: 1582-1590.

Buchholz CJ, Spehner D, Drillien R, Neubert WJ, Homann HE (1993) The conserved N-terminal region of Sendai virus nucleocapsid protein NP is required for nucleocapsid assembly. *J. Virol.* 67: 5803-5812.

Cantell K, Hirvonen S (1981) Preparation and assay of Sendai virus. *Methods Enzymol.* 78: 299-301.

Cantell K, Hirvonen S, Kauppinen HL, Myllyla G (1981) Production of interferon in human leukocytes from normal donors with the use of Sendai virus. *Methods Enzymol.* 78: 29-38.

Chattopadhyay S, Yamashita M, Zhang Y, Sen GC (2011) The IRF-3/Bax-mediated apoptotic pathway, activated by viral cytoplasmic RNA and DNA, inhibits virus replication. *J. Virol.* 85: 3708-3716.

Chaudhary PM, Ferguson C, Nguyen V, Nguyen O, Massa HF, Eby M, Jasmin A, Trask BJ, Hood L, Nelson PS (1998) Cloning and characterization of two Toll/Interleukin-1 receptor-like genes TIL3 and TIL4: evidence for a multi-gene receptor family in humans. *Blood* 91: 4020-4027.

Childs K, Stock N, Ross C, Andrejeva J, Hilton L, Skinner M, Randall R, Goodbourn S (2007) mda-5, but not RIG-I, is a common target for paramyxovirus V proteins. *Virology* 359: 190-200.

Choi MK, Wang Z, Ban T, Yanai H, Lu Y, Koshiba R, Nakaima Y, Hangai S, Savitsky D, Nakasato M, Negishi H, Takeuchi O, Honda K, Akira S, Tamura T, Taniguchi T (2009) A selective contribution of the RIG-I-like receptor pathway to type I interferon responses activated by cytosolic DNA. *Proc. Natl. Acad. Sci. U. S. A.* 106: 17870-17875.

Chu VC, Whittaker GR (2004) Influenza virus entry and infection require host cell N-linked glycoprotein. *Proc. Natl. Acad. Sci. U. S. A.* 101: 18153-18158.

Collins SE, Noyce RS, Mossman KL (2004) Innate cellular response to virus particle entry requires IRF3 but not virus replication. *J. Virol.* 78: 1706-1717.

Cox R, Plemper RK (2015) The paramyxovirus polymerase complex as a target for next-generation anti-paramyxovirus therapeutics. *Front. Microbiol.* 6: 459.

Curran J, Boeck R, Kolakofsky D (1991) The Sendai virus P gene expresses both an essential protein and an inhibitor of RNA synthesis by shuffling modules via mRNA editing. *Embo J.* 10: 3079-3085.

Curran J, Kolakofsky D (1988) Ribosomal initiation from an ACG codon in the Sendai virus P/C mRNA. *Embo J.* 7: 245-251.

Curran J, Marq JB, Kolakofsky D (1995) An N-terminal domain of the Sendai paramyxovirus P protein acts as a chaperone for the NP protein during the nascent chain assembly step of genome replication. *J. Virol.* 69: 849-855.

Darnell JE,Jr, Kerr IM, Stark GR (1994) Jak-STAT pathways and transcriptional activation in response to IFNs and other extracellular signaling proteins. *Science* 264: 1415-1421.

Deng H, Liu R, Ellmeier W, Choe S, Unutmaz D, Burkhart M, Di Marzio P, Marmon S, Sutton RE, Hill CM, Davis CB, Peiper SC, Schall TJ, Littman DR, Landau NR (1996) Identification of a major co-receptor for primary isolates of HIV-1. *Nature* 381: 661-666.

Der SD, Yang YL, Weissmann C, Williams BR (1997) A double-stranded RNA-activated protein kinase-dependent pathway mediating stress-induced apoptosis. *Proc. Natl. Acad. Sci. U. S. A.* 94: 3279-3283.

Der SD, Zhou A, Williams BR, Silverman RH (1998) Identification of genes differentially regulated by interferon alpha, beta, or gamma using oligonucleotide arrays. *Proc. Natl. Acad. Sci. U. S. A.* 95: 15623-15628.

Dethlefsen L, Kolakofsky D (1983) In vitro synthesis of the nonstructural C protein of Sendai virus. *J. Virol.* 46: 321-324.

Faísca P, Desmecht D (2007) Sendai virus, the mouse parainfluenza type 1: a longstanding pathogen that remains up-to-date. *Res. Vet. Sci.* 82: 115-125.

Feng Q, Hato SV, Langereis MA, Zoll J, Virgen-Slane R, Peisley A, Hur S, Semler BL, van Rij RP, van Kuppeveld FJ (2012) MDA5 detects the double-stranded RNA replicative form in picornavirus-infected cells. *Cell. Rep.* 2: 1187-1196.

Fensterl V, Sen GC (2009) Interferons and viral infections. *Biofactors* 35: 14-20.

Firquet S, Beaujard S, Lobert PE, Sane F, Caloone D, Izard D, Hober D (2015) Survival of Enveloped and Non-Enveloped Viruses on Inanimate Surfaces. *Microbes Environ.* 30: 140-144.

Fitzgerald KA, McWhirter SM, Faia KL, Rowe DC, Latz E, Golenbock DT, Coyle AJ, Liao SM, Maniatis T (2003) IKKepsilon and TBK1 are essential components of the IRF3 signaling pathway. *Nat. Immunol.* 4: 491-496.

Fritz JH, Le Bourhis L, Sellge G, Magalhaes JG, Fsihi H, Kufer TA, Collins C, Viala J, Ferrero RL, Girardin SE, Philpott DJ (2007) Nod1-mediated innate

immune recognition of peptidoglycan contributes to the onset of adaptive immunity. *Immunity* 26: 445-459.

Génin P, Algarte M, Roof P, Lin R, Hiscott J (2000) Regulation of RANTES chemokine gene expression requires cooperativity between NF-kappa B and IFN-regulatory factor transcription factors. *J. Immunol.* 164: 5352-5361.

Gorman WL, Gill DS, Scroggs RA, Portner A (1990) The hemagglutinin-neuraminidase glycoproteins of human parainfluenza virus type 1 and Sendai virus have high structure-function similarity with limited antigenic cross-reactivity. *Virology* 175: 211-221.

Grandvaux N, Servant MJ, tenOever B, Sen GC, Balachandran S, Barber GN, Lin R, Hiscott J (2002) Transcriptional profiling of interferon regulatory factor 3 target genes: direct involvement in the regulation of interferon-stimulated genes. *J. Virol.* 76: 5532-5539.

Gubbay O, Curran J, Kolakofsky D (2001) Sendai virus genome synthesis and assembly are coupled: a possible mechanism to promote viral RNA polymerase processivity. *J. Gen. Virol.* 82: 2895-2903.

Harder J, Bartels J, Christophers E, Schroder JM (2001) Isolation and characterization of human beta -defensin-3, a novel human inducible peptide antibiotic. *J. Biol. Chem.* 276: 5707-5713.

Hare D, Mossman KL (2013) Novel paradigms of innate immune sensing of viral infections. *Cytokine* 63: 219-224.

Hayashi F, Smith KD, Ozinsky A, Hawn TR, Yi EC, Goodlett DR, Eng JK, Akira S, Underhill DM, Aderem A (2001) The innate immune response to bacterial flagellin is mediated by Toll-like receptor 5. *Nature* 410: 1099-1103.

Horikami SM, Curran J, Kolakofsky D, Moyer SA (1992) Complexes of Sendai virus NP-P and P-L proteins are required for defective interfering particle genome replication in vitro. *J. Virol.* 66: 4901-4908.

Horikami SM, Hector RE, Smallwood S, Moyer SA (1997) The Sendai virus C protein binds the L polymerase protein to inhibit viral RNA synthesis. *Virology* 235: 261-270.

Hornung V, Ellegast J, Kim S, Brzozka K, Jung A, Kato H, Poeck H, Akira S, Conzelmann KK, Schlee M, Endres S, Hartmann G (2006) 5'-Triphosphate RNA is the ligand for RIG-I. *Science* 314: 994-997.

Hornung V, Schlender J, Guenthner-Biller M, Rothenfusser S, Endres S, Conzelmann KK, Hartmann G (2004) Replication-dependent potent IFN-alpha induction in human plasmacytoid dendritic cells by a single-stranded RNA virus. *J. Immunol.* 173: 5935-5943.

Hoshino K, Takeuchi O, Kawai T, Sanjo H, Ogawa T, Takeda Y, Takeda K, Akira S (1999) Cutting edge: Toll-like receptor 4 (TLR4)-deficient mice are hyporesponsive to lipopolysaccharide: evidence for TLR4 as the Lps gene product. *J. Immunol.* 162: 3749-3752.

Hwang SY, Hertzog PJ, Holland KA, Sumarsono SH, Tymms MJ, Hamilton JA, Whitty G, Bertoncello I, Kola I (1995) A null mutation in the gene encoding

a type I interferon receptor component eliminates antiproliferative and antiviral responses to interferons alpha and beta and alters macrophage responses. *Proc. Natl. Acad. Sci. U. S. A.* 92: 11284-11288.

Irie T, Kiyotani K, Igarashi T, Yoshida A, Sakaguchi T (2012) Inhibition of interferon regulatory factor 3 activation by paramyxovirus V protein. *J. Virol.* 86: 7136-7145.

Irie T, Nagata N, Yoshida T, Sakaguchi T (2008) Recruitment of Alix/AIP1 to the plasma membrane by Sendai virus C protein facilitates budding of virus-like particles. *Virology* 371: 108-120.

Irie T, Okamoto I, Yoshida A, Nagai Y, Sakaguchi T (2014) Sendai virus C proteins regulate viral genome and antigenome synthesis to dictate the negative genome polarity. *J. Virol.* 88: 690-698.

Irie T, Shimazu Y, Yoshida T, Sakaguchi T (2007) The YLDL sequence within Sendai virus M protein is critical for budding of virus-like particles and interacts with Alix/AIP1 independently of C protein. *J. Virol.* 81: 2263-2273.

Ishida N, Homma M (1978) Sendai virus. *Adv. Virus Res.* 23: 349-383.

Iverson LE, Rose JK (1981) Localized attenuation and discontinuous synthesis during vesicular stomatitis virus transcription. *Cell* 23: 477-484.

Jewell NA, Vaghefi N, Mertz SE, Akter P, Peebles RS,Jr, Bakaletz LO, Durbin RK, Flano E, Durbin JE (2007) Differential type I interferon induction by respiratory syncytial virus and influenza a virus in vivo. *J. Virol.* 81: 9790-9800.

Jiang M, Österlund P, Sarin LP, Poranen MM, Bamford DH, Guo D, Julkunen I (2011) Innate immune responses in human monocyte-derived dendritic cells are highly dependent on the size and the 5' phosphorylation of RNA molecules. *J. Immunol.* 187: 1713-1721.

Jin CH, Kusuhara K, Yonemitsu Y, Nomura A, Okano S, Takeshita H, Hasegawa M, Sueishi K, Hara T (2003) Recombinant Sendai virus provides a highly efficient gene transfer into human cord blood-derived hematopoietic stem cells. *Gene Ther.* 10: 272-277.

Jin HS, Suh HW, Kim SJ, Jo EK (2017) Mitochondrial Control of Innate Immunity and Inflammation. *Immune Netw.* 17: 77-88.

Juang YT, Lowther W, Kellum M, Au WC, Lin R, Hiscott J, Pitha PM (1998) Primary activation of interferon A and interferon B gene transcription by interferon regulatory factor 3. *Proc. Natl. Acad. Sci. U. S. A.* 95: 9837-9842.

Kato A, Cortese-Grogan C, Moyer SA, Sugahara F, Sakaguchi T, Kubota T, Otsuki N, Kohase M, Tashiro M, Nagai Y (2004) Characterization of the amino acid residues of sendai virus C protein that are critically involved in its interferon antagonism and RNA synthesis down-regulation. *J. Virol.* 78: 7443-7454.

Kato A, Kiyotani K, Sakai Y, Yoshida T, Nagai Y (1997) The paramyxovirus, Sendai virus, V protein encodes a luxury function required for viral pathogenesis. *Embo J.* 16: 578-587.

Kato A, Ohnishi Y, Kohase M, Saito S, Tashiro M, Nagai Y (2001) Y2, the smallest of the Sendai virus C proteins, is fully capable of both counteracting the antiviral action of interferons and inhibiting viral RNA synthesis. *J. Virol.* 75: 3802-3810.

Kato H, Sato S, Yoneyama M, Yamamoto M, Uematsu S, Matsui K, Tsujimura T, Takeda K, Fujita T, Takeuchi O, Akira S (2005) Cell type-specific involvement of RIG-I in antiviral response. *Immunity* 23: 19-28.

Kato H, Takeuchi O, Sato S, Yoneyama M, Yamamoto M, Matsui K, Uematsu S, Jung A, Kawai T, Ishii KJ, Yamaguchi O, Otsu K, Tsujimura T, Koh CH, Reis e Sousa C, Matsuura Y, Fujita T, Akira S (2006) Differential roles of MDA5 and RIG-I helicases in the recognition of RNA viruses. *Nature* 441: 101-105.

Kawai T, Takahashi K, Sato S, Coban C, Kumar H, Kato H, Ishii KJ, Takeuchi O, Akira S (2005) IPS-1, an adaptor triggering RIG-I- and Mda5-mediated type I interferon induction. *Nat. Immunol.* 6: 981-988.

Kido H, Yokogoshi Y, Sakai K, Tashiro M, Kishino Y, Fukutomi A, Katunuma N (1992) Isolation and characterization of a novel trypsin-like protease found in rat bronchiolar epithelial Clara cells. A possible activator of the viral fusion glycoprotein. *J. Biol. Chem.* 267: 13573-13579.

Kolakofsky D, Le Mercier P, Iseni F, Garcin D (2004) Viral DNA polymerase scanning and the gymnastics of Sendai virus RNA synthesis. *Virology* 318: 463-473.

Komatsu T, Takeuchi K, Yokoo J, Gotoh B (2004) C and V proteins of Sendai virus target signaling pathways leading to IRF-3 activation for the negative regulation of interferon-beta production. *Virology* 325: 137-148.

Konno H, Yamamoto T, Yamazaki K, Gohda J, Akiyama T, Semba K, Goto H, Kato A, Yujiri T, Imai T, Kawaguchi Y, Su B, Takeuchi O, Akira S, Tsunetsugu-Yokota Y, Inoue J (2009) TRAF6 establishes innate immune responses by activating NF-kappaB and IRF7 upon sensing cytosolic viral RNA and DNA. *PLoS One* 4.

Koonin EV, Dolja VV, Krupovic M (2015) Origins and evolution of viruses of eukaryotes: The ultimate modularity. *Virology* 479-480: 2-25.

Koonin EV, Senkevich TG, Dolja VV (2006) The ancient Virus World and evolution of cells. *Biol. Direct* 1.

Kotenko SV, Gallagher G, Baurin VV, Lewis-Antes A, Shen M, Shah NK, Langer JA, Sheikh F, Dickensheets H, Donnelly RP (2003) IFN-lambdas mediate antiviral protection through a distinct class II cytokine receptor complex. *Nat. Immunol.* 4: 69-77.

Koyama AH, Irie H, Kato A, Nagai Y, Adachi A (2003) Virus multiplication and induction of apoptosis by Sendai virus: role of the C proteins. *Microbes Infect.* 5: 373-378.

Kramer A, Schwebke I, Kampf G (2006) How long do nosocomial pathogens persist on inanimate surfaces? A systematic review. *BMC Infect. Dis.* 6

La Scola B, Desnues C, Pagnier I, Robert C, Barrassi L, Fournous G, Merchat M, Suzan-Monti M, Forterre P, Koonin E, Raoult D (2008) The virophage as a unique parasite of the giant mimivirus. *Nature* 455: 100-104.

LaFleur DW, Nardelli B, Tsareva T, Mather D, Feng P, Semenuk M, Taylor K, Buergin M, Chinchilla D, Roshke V, Chen G, Ruben SM, Pitha PM, Coleman TA, Moore PA (2001) Interferon-kappa, a novel type I interferon expressed in human keratinocytes. *J. Biol. Chem.* 276: 39765-39771.

Lee NR, Kim HI, Choi MS, Yi CM, Inn KS (2015) Regulation of MDA5-MAVS Antiviral Signaling Axis by TRIM25 through TRAF6-Mediated NF-kappaB Activation. *Mol. Cells* 38: 759-764.

Leppert M, Rittenhouse L, Perrault J, Summers DF, Kolakofsky D (1979) Plus and minus strand leader RNAs in negative strand virus-infected cells. *Cell* 18: 735-747.

Li W, Hofer MJ, Songkhunawej P, Jung SR, Hancock D, Denyer G, Campbell IL (2017) Type I interferon-regulated gene expression and signaling in murine mixed glial cells lacking signal transducers and activators of transcription 1 or 2 or interferon regulatory factor 9. *J. Biol. Chem.* 292: 5845-5859.

Liemann S, Chandran K, Baker TS, Nibert ML, Harrison SC (2002) Structure of the reovirus membrane-penetration protein, Mu1, in a complex with is protector protein, Sigma3. *Cell* 108: 283-295.

Lin R, Genin P, Mamane Y, Hiscott J (2000) Selective DNA binding and association with the CREB binding protein coactivator contribute to differential activation of alpha/beta interferon genes by interferon regulatory factors 3 and 7. *Mol. Cell. Biol.* 20: 6342-6353.

Lin R, Heylbroeck C, Genin P, Pitha PM, Hiscott J (1999) Essential role of interferon regulatory factor 3 in direct activation of RANTES chemokine transcription. *Mol. Cell. Biol.* 19: 959-966.

Lin R, Heylbroeck C, Pitha PM, Hiscott J (1998) Virus-dependent phosphorylation of the IRF-3 transcription factor regulates nuclear translocation, transactivation potential, and proteasome-mediated degradation. *Mol. Cell. Biol.* 18: 2986-2996.

Lin R, Mamane Y, Hiscott J (1999) Structural and functional analysis of interferon regulatory factor 3: localization of the transactivation and autoinhibitory domains. *Mol. Cell. Biol.* 19: 2465-2474.

Liu G, Lu Y, Thulasi Raman SN, Xu F, Wu Q, Li Z, Brownlie R, Liu Q, Zhou Y (2018) Nuclear-resident RIG-I senses viral replication inducing antiviral immunity. *Nat. Commun.* 9.

Livak KJ, Schmittgen TD (2001) Analysis of relative gene expression data using real-time quantitative PCR and the $2^{-\Delta\Delta CT}$ Method. *Methods* 25: 402-408.

Loo YM, Fornek J, Crochet N, Bajwa G, Perwitasari O, Martinez-Sobrido L, Akira S, Gill MA, Garcia-Sastre A, Katze MG, Gale M,Jr (2008) Distinct RIG-

I and MDA5 signaling by RNA viruses in innate immunity. *J. Virol.* 82: 335-345.

Lovinger GG, Ling HP, Gilden RV, Hatanaka M (1975) Effect of UV Light on RNA-Directed DNA Polymerase Activity of Murine Oncornaviruses. *J. Virol.* 15: 1273-1275.

Lyn D, Gill DS, Scroggs RA, Portner A (1991) The nucleoproteins of human parainfluenza virus type 1 and Sendai virus share amino acid sequences and antigenic and structural determinants. *J. Gen. Virol.* 72: 983-987.

Markwell MA, Paulson JC (1980) Sendai virus utilizes specific sialyloligosaccharides as host cell receptor determinants. *Proc. Natl. Acad. Sci. U. S. A.* 77: 5693-5697.

Mateu MG (2013) Assembly, stability and dynamics of virus capsids. *Arch. Biochem. Biophys.* 531: 65-79.

Matlin KS, Reggio H, Helenius A, Simons K (1981) Infectious entry pathway of influenza virus in a canine kidney cell line. *J. Cell Biol.* 91: 601-613.

Matsumoto T, Maeno K (1961) Growth of HVJ (hemagglutinating virus of Japan) in mouse lung cells. *Jpn. J. Microbiol.* 5: 89-96.

Matveeva OV, Guo ZS, Shabalina SA, Chumakov PM (2015) Oncolysis by paramyxoviruses: multiple mechanisms contribute to therapeutic efficiency. *Mol. Ther. Oncolytics* 2.

McWhirter SM, Fitzgerald KA, Rosains J, Rowe DC, Golenbock DT, Maniatis T (2004) IFN-regulatory factor 3-dependent gene expression is defective in Tbk1-deficient mouse embryonic fibroblasts. *Proc. Natl. Acad. Sci. U. S. A.* 101: 233-238.

Medzhitov R (2007) Recognition of microorganisms and activation of the immune response. *Nature* 449: 819-826.

Medzhitov R, Preston-Hurlburt P, Janeway CA,Jr (1997) A human homologue of the Drosophila Toll protein signals activation of adaptive immunity. *Nature* 388: 394-397.

Melchjorsen J, Jensen SB, Malmgaard L, Rasmussen SB, Weber F, Bowie AG, Matikainen S, Paludan SR (2005) Activation of innate defense against a paramyxovirus is mediated by RIG-I and TLR7 and TLR8 in a cell-type-specific manner. *J. Virol.* 79: 12944-12951.

Meraz MA, White JM, Sheehan KC, Bach EA, Rodig SJ, Dighe AS, Kaplan DH, Riley JK, Greenlund AC, Campbell D, Carver-Moore K, DuBois RN, Clark R, Aguet M, Schreiber RD (1996) Targeted disruption of the Stat1 gene in mice reveals unexpected physiologic specificity in the JAK-STAT signaling pathway. *Cell* 84: 431-442.

Meylan E, Tschopp J, Karin M (2006) Intracellular pattern recognition receptors in the host response. *Nature* 442: 39-44.

Miller RL, Plagemann PG (1974) Effect of ultraviolet light on mengovirus: formation of uracil dimers, instability and degradation of capsid, and covalent linkage of protein to viral RNA. *J. Virol.* 13: 729-739.

Mogensen TH, Paludan SR (2005) Reading the viral signature by Toll-like receptors and other pattern recognition receptors. *J. Mol. Med.* 83: 180-192.

Moscufo N, Yafal AG, Rogove A, Hogle J, Chow M (1993) A mutation in VP4 defines a new step in the late stages of cell entry by poliovirus. *J. Virol.* 67: 5075-5078.

Müller M, Laxton C, Briscoe J, Schindler C, Improta T, Darnell JE,Jr, Stark GR, Kerr IM (1993) Complementation of a mutant cell line: central role of the 91 kDa polypeptide of ISGF3 in the interferon-alpha and -gamma signal transduction pathways. *Embo J.* 12: 4221-4228.

Müller U, Steinhoff U, Reis LF, Hemmi S, Pavlovic J, Zinkernagel RM, Aguet M (1994) Functional role of type I and type II interferons in antiviral defense. *Science* 264: 1918-1921.

Murphy MF, Lazzarini RA (1974) Synthesis of viral mRNA and polyadenylate by a ribonucleoprotein complex from extracts of VSV-infected cells. *Cell* 3: 77-84.

Myers TM, Moyer SA (1997) An amino-terminal domain of the Sendai virus nucleocapsid protein is required for template function in viral RNA synthesis. *J. Virol.* 71: 918-924.

Nakanishi M, Otsu M (2012) Development of Sendai virus vectors and their potential applications in gene therapy and regenerative medicine. *Curr. Gene Ther.* 12: 410-416.

Nguyen KB, Salazar-Mather TP, Dalod MY, Van Deusen JB, Wei XQ, Liew FY, Caligiuri MA, Durbin JE, Biron CA (2002) Coordinated and distinct roles for IFN-alpha beta, IL-12, and IL-15 regulation of NK cell responses to viral infection. *J. Immunol.* 169: 4279-4287.

Noton SL, Fearns R (2015) Initiation and regulation of paramyxovirus transcription and replication. *Virology* 479-480: 545-554.

Noton SL, Tremaglio CZ, Fearns R (2019) Killing two birds with one stone: How the respiratory syncytial virus polymerase initiates transcription and replication. *PLoS Pathog.* 15.

Novick D, Cohen B, Rubinstein M (1994) The human interferon alpha/beta receptor: characterization and molecular cloning. *Cell* 77: 391-400.

Ogino T, Kobayashi M, Iwama M, Mizumoto K (2005) Sendai virus RNA-dependent RNA polymerase L protein catalyzes cap methylation of virus-specific mRNA. *J. Biol. Chem.* 280: 4429-4435.

Oh SW, Onomoto K, Wakimoto M, Onoguchi K, Ishidate F, Fujiwara T, Yoneyama M, Kato H, Fujita T (2016) Leader-Containing Uncapped Viral Transcript Activates RIG-I in Antiviral Stress Granules. *PLoS Pathog.* 12.

Okada Y, Murayama F, Yamada K (1966) Requirement of energy for the cell fusion reaction of Ehrlich ascites tumor cells by HVJ. *Virology* 28: 115-130.

Ozinsky A, Underhill DM, Fontenot JD, Hajjar AM, Smith KD, Wilson CB, Schroeder L, Aderem A (2000) The repertoire for pattern recognition of pathogens by the innate immune system is defined by cooperation between toll-like receptors. *Proc. Natl. Acad. Sci. U. S. A.* 97: 13766-13771.

Park A, Hong P, Won ST, Thibault PA, Vigant F, Oguntuyo KY, Taft JD, Lee B (2016) Sendai virus, an RNA virus with no risk of genomic integration, delivers CRISPR/Cas9 for efficient gene editing. *Mol. Ther. Methods Clin. Dev.* 3: 16057.

Park C, Li S, Cha E, Schindler C (2000) Immune response in Stat2 knockout mice. *Immunity* 13: 795-804.

Pavlovic J, Zurcher T, Haller O, Staeheli P (1990) Resistance to influenza virus and vesicular stomatitis virus conferred by expression of human MxA protein. *J. Virol.* 64: 3370-3375.

Peters K, Chattopadhyay S, Sen GC (2008) IRF-3 activation by Sendai virus infection is required for cellular apoptosis and avoidance of persistence. *J. Virol.* 82: 3500-3508.

Plemper RK (2011) Cell entry of enveloped viruses. *Curr. Opin. Virol.* 1: 92-100.

Poch O, Sauvaget I, Delarue M, Tordo N (1989) Identification of four conserved motifs among the RNA-dependent polymerase encoding elements. *Embo J.* 8: 3867-3874.

Poole E, He B, Lamb RA, Randall RE, Goodbourn S (2002) The V proteins of simian virus 5 and other paramyxoviruses inhibit induction of interferon-beta. *Virology* 303: 33-46.

Portner A, Murti KG, Morgan EM, Kingsbury DW (1988) Antibodies against Sendai virus L protein: distribution of the protein in nucleocapsids revealed by immunoelectron microscopy. *Virology* 163: 236-239.

Pridgen C, Kingsbury DW (1972) Adenylate-rich sequences in Sendai virus transcripts from infected cells. *J. Virol.* 10: 314-317.

Prokunina-Olsson L, Muchmore B, Tang W, Pfeiffer RM, Park H, Dickensheets H, Hergott D, Porter-Gill P, Mumy A, Kohaar I, Chen S, Brand N, Tarway M, Liu L, Sheikh F, Astemborski J, Bonkovsky HL, Edlin BR, Howell CD, Morgan TR, Thomas DL, Rehermann B, Donnelly RP, O'Brien TR (2013) A variant upstream of IFNL3 (IL28B) creating a new interferon gene IFNL4 is associated with impaired clearance of hepatitis C virus. *Nat. Genet.* 45: 164-171.

Rakoff-Nahoum S, Paglino J, Eslami-Varzaneh F, Edberg S, Medzhitov R (2004) Recognition of commensal microflora by toll-like receptors is required for intestinal homeostasis. *Cell* 118: 229-241.

Robinson WS (1971) Sendai virus RNA synthesis and nucleocapsid formation in the presence of cycloheximide. *Virology* 44: 494-502.

Rock FL, Hardiman G, Timans JC, Kastelein RA, Bazan JF (1998) A family of human receptors structurally related to Drosophila Toll. *Proc. Natl. Acad. Sci. U. S. A.* 95: 588-593.

Saha SK, Pietras EM, He JQ, Kang JR, Liu SY, Oganesyan G, Shahangian A, Zarnegar B, Shiba TL, Wang Y, Cheng G (2006) Regulation of antiviral responses by a direct and specific interaction between TRAF3 and Cardif. *Embo J.* 25: 3257-3263.

Saito T, Hirai R, Loo YM, Owen D, Johnson CL, Sinha SC, Akira S, Fujita T, Gale M,Jr (2007) Regulation of innate antiviral defenses through a shared repressor domain in RIG-I and LGP2. *Proc. Natl. Acad. Sci. U. S. A.* 104: 582-587.

Sanghavi SK, Shankarappa R, Reinhart TA (2004) Genetic analysis of Toll/Interleukin-1 Receptor (TIR) domain sequences from rhesus macaque Toll-like receptors (TLRs) 1-10 reveals high homology to human TLR/TIR sequences. *Immunogenetics* 56: 667-674.

Sato M, Suemori H, Hata N, Asagiri M, Ogasawara K, Nakao K, Nakaya T, Katsuki M, Noguchi S, Tanaka N, Taniguchi T (2000) Distinct and essential roles of transcription factors IRF-3 and IRF-7 in response to viruses for IFN-alpha/beta gene induction. *Immunity* 13: 539-548.

Sato M, Tanaka N, Hata N, Oda E, Taniguchi T (1998) Involvement of the IRF family transcription factor IRF-3 in virus-induced activation of the IFN-beta gene. *FEBS Lett.* 425: 112-116.

Scheid A, Choppin PW (1974) Identification of biological activities of paramyxovirus glycoproteins. Activation of cell fusion, hemolysis, and infectivity of proteolytic cleavage of an inactive precursor protein of Sendai virus. *Virology* 57: 475-490.

Scheid A, Choppin PW (1977) Two disulfide-linked polypeptide chains constitute the active F protein of paramyxoviruses. *Virology* 80: 54-66.

Schindler C, Shuai K, Prezioso VR, Darnell JE,Jr (1992) Interferon-dependent tyrosine phosphorylation of a latent cytoplasmic transcription factor. *Science* 257: 809-813.

Schlee M, Roth A, Hornung V, Hagmann CA, Wimmenauer V, Barchet W, Coch C, Janke M, Mihailovic A, Wardle G, Juranek S, Kato H, Kawai T, Poeck H, Fitzgerald KA, Takeuchi O, Akira S, Tuschl T, Latz E, Ludwig J, Hartmann G (2009) Recognition of 5' triphosphate by RIG-I helicase requires short blunt double-stranded RNA as contained in panhandle of negative-strand virus. *Immunity* 31: 25-34.

Schneider-Poetsch T, Ju J, Eyler DE, Dang Y, Bhat S, Merrick WC, Green R, Shen B, Liu JO (2010) Inhibition of eukaryotic translation elongation by cycloheximide and lactimidomycin. *Nat. Chem. Biol.* 6: 209-217.

Servant MJ, ten Oever B, LePage C, Conti L, Gessani S, Julkunen I, Lin R, Hiscott J (2001) Identification of distinct signaling pathways leading to the phosphorylation of interferon regulatory factor 3. *J. Biol. Chem.* 276: 355-363.

Seth RB, Sun L, Ea CK, Chen ZJ (2005) Identification and characterization of MAVS, a mitochondrial antiviral signaling protein that activates NF-kappaB and IRF 3. *Cell* 122: 669-682.

Sharma S, tenOever BR, Grandvaux N, Zhou GP, Lin R, Hiscott J (2003) Triggering the interferon antiviral response through an IKK-related pathway. *Science* 300: 1148-1151.

Shirai J, Kanno T, Tsuchiya Y, Mitsubayashi S, Seki R (2000) Effects of chlorine, iodine, and quaternary ammonium compound disinfectants on several exotic disease viruses. *J. Vet. Med. Sci.* 62: 85-92.

Shuai K, Horvath CM, Huang LH, Qureshi SA, Cowburn D, Darnell JE,Jr (1994) Interferon activation of the transcription factor Stat91 involves dimerization through SH2-phosphotyrosyl peptide interactions. *Cell* 76: 821-828.

Slobod KS, Shenep JL, Lujan-Zilbermann J, Allison K, Brown B, Scroggs RA, Portner A, Coleclough C, Hurwitz JL (2004) Safety and immunogenicity of intranasal murine parainfluenza virus type 1 (Sendai virus) in healthy human adults. *Vaccine* 22: 3182-3186.

Smallwood S, Ryan KW, Moyer SA (1994) Deletion analysis defines a carboxyl-proximal region of Sendai virus P protein that binds to the polymerase L protein. *Virology* 202: 154-163.

Sokol CL, Luster AD (2015) The chemokine system in innate immunity. *Cold Spring Harb Perspect. Biol.* 7.

Strähle L, Garcin D, Le Mercier P, Schlaak JF, Kolakofsky D (2003) Sendai virus targets inflammatory responses, as well as the interferon-induced antiviral state, in a multifaceted manner. *J. Virol.* 77: 7903-7913.

Takahasi K, Yoneyama M, Nishihori T, Hirai R, Kumeta H, Narita R, Gale M,Jr, Inagaki F, Fujita T (2008) Nonself RNA-sensing mechanism of RIG-I helicase and activation of antiviral immune responses. *Mol. Cell* 29: 428-440.

Takaoka A, Yanai H (2006) Interferon signalling network in innate defence. *Cell. Microbiol.* 8: 907-922.

Takimoto T, Murti KG, Bousse T, Scroggs RA, Portner A (2001) Role of matrix and fusion proteins in budding of Sendai virus. *J. Virol.* 75: 11384-11391.

Tanabayashi K, Compans RW (1996) Functional interaction of paramyxovirus glycoproteins: identification of a domain in Sendai virus HN which promotes cell fusion. *J. Virol.* 70: 6112-6118.

Tashiro M, Yamakawa M, Tobita K, Klenk HD, Rott R, Seto JT (1990) Organ tropism of Sendai virus in mice: proteolytic activation of the fusion glycoprotein in mouse organs and budding site at the bronchial epithelium. *J. Virol.* 64: 3627-3634.

Taylor PR, Tsoni SV, Willment JA, Dennehy KM, Rosas M, Findon H, Haynes K, Steele C, Botto M, Gordon S, Brown GD (2007) Dectin-1 is required for

beta-glucan recognition and control of fungal infection. *Nat. Immunol.* 8: 31-38.

Thevenin T, Lobert PE, Hober D (2013) Inactivation of coxsackievirus B4, feline calicivirus and herpes simplex virus type 1: unexpected virucidal effect of a disinfectant on a non-enveloped virus applied onto a surface. *Intervirology* 56: 224-230.

Toni LS, Garcia AM, Jeffrey DA, Jiang X, Stauffer BL, Miyamoto SD, Sucharov CC (2018) Optimization of phenol-chloroform RNA extraction. *MethodsX* 5: 599-608.

Tordo N, Poch O, Ermine A, Keith G, Rougeon F (1988) Completion of the rabies virus genome sequence determination: highly conserved domains among the L (polymerase) proteins of unsegmented negative-strand RNA viruses. *Virology* 165: 565-576.

Tovey MG, Streuli M, Gresser I, Gugenheim J, Blanchard B, Guymarho J, Vignaux F, Gigou M (1987) Interferon messenger RNA is produced constitutively in the organs of normal individuals. *Proc. Natl. Acad. Sci. U. S. A.* 84: 5038-5042.

Uchida L, Espada-Murao LA, Takamatsu Y, Okamoto K, Hayasaka D, Yu F, Nabeshima T, Buerano CC, Morita K (2014) The dengue virus conceals double-stranded RNA in the intracellular membrane to escape from an interferon response. *Sci. Rep.* 4: 7395.

Urban MB, Schreck R, Baeuerle PA (1991) NF-kappa B contacts DNA by a heterodimer of the p50 and p65 subunit. *Embo J.* 10: 1817-1825.

Vabret N, Blander JM (2013) Sensing microbial RNA in the cytosol. *Front. Immunol.* 4: 468.

Veals SA, Santa Maria T, Levy DE (1993) Two domains of ISGF3 gamma that mediate protein-DNA and protein-protein interactions during transcription factor assembly contribute to DNA-binding specificity. *Mol. Cell. Biol.* 13: 196-206.

Veals SA, Schindler C, Leonard D, Fu XY, Aebersold R, Darnell JE,Jr, Levy DE (1992) Subunit of an alpha-interferon-responsive transcription factor is related to interferon regulatory factor and Myb families of DNA-binding proteins. *Mol. Cell. Biol.* 12: 3315-3324.

Veckman V, Österlund P, Fagerlund R, Melen K, Matikainen S, Julkunen I (2006) TNF-alpha and IFN-alpha enhance influenza-A-virus-induced chemokine gene expression in human A549 lung epithelial cells. *Virology* 345: 96-104.

Vidal S, Curran J, Kolakofsky D (1990) A stuttering model for paramyxovirus P mRNA editing. *Embo J.* 9: 2017-2022.

Walsh D, Mohr I (2011) Viral subversion of the host protein synthesis machinery. *Nat. Rev. Microbiol.* 9: 860-875.

Weber M, Gawanbacht A, Habjan M, Rang A, Borner C, Schmidt AM, Veitinger S, Jacob R, Devignot S, Kochs G, Garcia-Sastre A, Weber F (2013)

Incoming RNA virus nucleocapsids containing a 5'-triphosphorylated genome activate RIG-I and antiviral signaling. *Cell. Host Microbe* 13: 336-346.

Wettstein FO, Noll H, Penman S (1964) Effect of Cycloheximide on Ribosomal Aggregates Engaged in Protein Synthesis in Vitro. *Biochim. Biophys. Acta* 87: 525-528.

Wu J, Chen ZJ (2014) Innate immune sensing and signaling of cytosolic nucleic acids. *Annu. Rev. Immunol.* 32: 461-488.

Yonemitsu Y, Kitson C, Ferrari S, Farley R, Griesenbach U, Judd D, Steel R, Scheid P, Zhu J, Jeffery PK, Kato A, Hasan MK, Nagai Y, Masaki I, Fukumura M, Hasegawa M, Geddes DM, Alton EW (2000) Efficient gene transfer to airway epithelium using recombinant Sendai virus. *Nat. Biotechnol.* 18: 970-973.

Yoneyama M, Kikuchi M, Matsumoto K, Imaizumi T, Miyagishi M, Taira K, Foy E, Loo YM, Gale M,Jr, Akira S, Yonehara S, Kato A, Fujita T (2005) Shared and unique functions of the DExD/H-box helicases RIG-I, MDA5, and LGP2 in antiviral innate immunity. *J. Immunol.* 175: 2851-2858.

Yoneyama M, Kikuchi M, Natsukawa T, Shinobu N, Imaizumi T, Miyagishi M, Taira K, Akira S, Fujita T (2004) The RNA helicase RIG-I has an essential function in double-stranded RNA-induced innate antiviral responses. *Nat. Immunol.* 5: 730-737.

Yoneyama M, Suhara W, Fukuhara Y, Fukuda M, Nishida E, Fujita T (1998) Direct triggering of the type I interferon system by virus infection: activation of a transcription factor complex containing IRF-3 and CBP/p300. *Embo J.* 17: 1087-1095.

Zhou A, Paranjape J, Brown TL, Nie H, Naik S, Dong B, Chang A, Trapp B, Fairchild R, Colmenares C, Silverman RH (1997) Interferon action and apoptosis are defective in mice devoid of 2',5'-oligoadenylate-dependent RNase L. *Embo J.* 16: 6355-6363.

Zhu Y, Yao S, Chen L (2011) Cell surface signaling molecules in the control of immune responses: a tide model. *Immunity* 34: 466-478.

Österlund P, Veckman V, Siren J, Klucher KM, Hiscott J, Matikainen S, Julkunen I (2005) Gene expression and antiviral activity of alpha/beta interferons and interleukin-29 in virus-infected human myeloid dendritic cells. *J. Virol.* 79: 9608-9617.

Österlund PI, Pietila TE, Veckman V, Kotenko SV, Julkunen I (2007) IFN regulatory factor family members differentially regulate the expression of type III IFN (IFN-lambda) genes. *J. Immunol.* 179: 3434-3442.

Österlund P, Strengell M, Sarin LP, Poranen MM, Fagerlund R, Melen K, Julkunen I (2012) Incoming influenza A virus evades early host recognition, while influenza B virus induces interferon expression directly upon entry. *J. Virol.* 86: 11183-11193.

# 7. Appendices

1. The growth medium:

HAM'S F12 with 1 mM L-glutamine (Cytiva) medium supplemented with 10 % Fetal Bovine Serum (FBS) (Biowest) and 10 µg / ml of gentamycin sulphate (Biological Industries).

2. Protocol for detaching A549 cells:

Growth medium was poured out, and the flask was washed with RT-warmed (approximately 25 °C) Phosphate-buffered saline (PBS) (Cytiva). Cells were incubated with 1:1 solution of Versene (0,02 %, Lonza) and trypsin (0,25 %, Lonza) in 5 % $CO_2$ conditions at + 37 °C for approximately 10 min. Two volume of growth medium was added, the mixture was mixed briefly, and the cell number was enumerated with hemocytometer using Trypan blue staining (Bio-Rad) in 1:200 dilution in MQ.

3. HAM's F12 medium:

HAM'S F12 with 1 mM L-Glutamine (Cytiva) medium.

4. 1x DMEM medium:

1x Dulbecco's modified Eagle's (DMEM) medium with 25 mM 4-(2-hydroxyethyl)-1-piperazineethanesulfonic acid (HEPES) and 4,5 g / l glucose (Lonza).

5. Complete membrane image of figure 8 that shows the expression of SeV proteins in infected A549 cells. The cells were infected with a SeV MOI 180 and at different time points (2h, 4h, 6h, 8h, 16h, 24h) they were lysed, and total proteins were collected. As a control, uninfected MOCK sample was also collected. Twenty µg of protein per sample were separated on an SDS-PAGE gel and transferred to a nitrocellulose membrane, which was stained with anti-SeV polyclonal antibody. The corresponding proteins are indicated with arrows on the right and the ladder bands of known sizes are presented on the left.
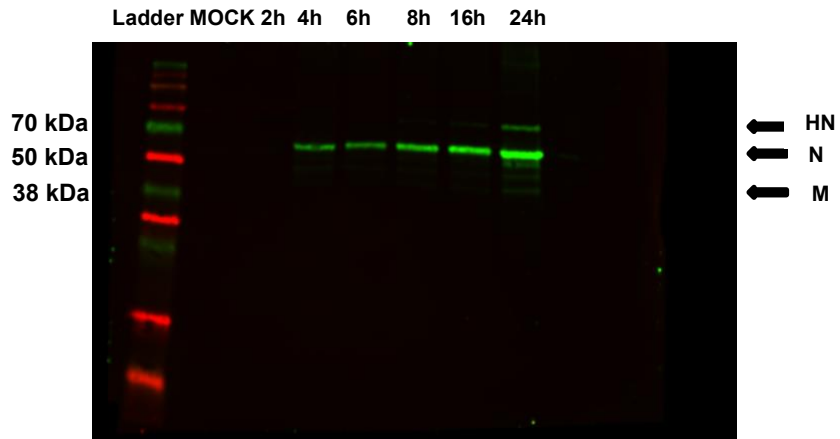
6. Complete membrane image of figure 9 that shows the expression of IRF3 in infected A549 cells. The cells were infected with SeV Cantell strain at a MOI 180 and at different time points (2h, 4h, 6h, 8h, 16h, 24h) the cells were lysed, and total proteins were collected. As a control, uninfected MOCK sample was also collected. From the samples, containing 20 µg of protein per sample, relative expression levels of IRF3 protein was analyzed by immunoblotting. The membrane was stained with anti-IRF3 monoclonal as well as with GAPDH that functioned as a loading control. The corresponding proteins are indicated with arrows on the right and the ladder bands of known sizes are presented on the left.